MTI 85TR28

HPOTP LOW-SPEED FLEXIBLE ROTOR BALANCING - PHASE I FINAL REPORT

Prepared by:

J. Giordano

E. Zorzi

Prepared for:

NASA Marshall Space Flight Center

Systems Dynamics Laboratory

23 July 1985

MTI 85TR28

HPOTP LOW-SPEED FLEXIBLE ROTOR BALANCING - PHASE I FINAL REPORT

Prepared by:

J. Giordano
E. Zorzi

Prepared for:

NASA Marshall Space Flight Center

Prepared under:

Contract No. NAS8-35598
MTI Project No. 0542-44550

23 July 1985

MECHANICAL TECHNOLOGY INCORPORATED
968 Albany-Shaker Road
Latham, New York 12110

TABLE OF CONTENTS

Section		Page
	LIST OF FIGURES	ii
	LIST OF TABLES	iv
1.0	INTRODUCTION	1-1
2.0	LOW-SPEED FLEXIBLE ROTOR BALANCING	2-1
	2.1 Formulation	2-1
	2.2 HPOTP Low-Speed Flexible Balancing Assessment	2-5
3.0	EMPIRICAL EVALUATION	3-1
	3.1 Test Rig Description	3-1
	3.2 Test Rig Analysis	3-11
	3.3 Test Results	3-19
4.0	CONCLUSIONS AND RECOMMENDATIONS	4-1
	4.1 Conclusions	4-1
	4.2 Recommendations	4-2
5.0	REFERENCES	5-1
	APPENDIX A	A-1

LIST OF FIGURES

Figure		Page
2-1	Required Number of Balance.....	2-3
2-2	HPOTP Balance Planes.....	2-6
2-3	HPOTP Mode Shapes.....	2-7
2-4	HPOTP Low-Speed Flexible Balancing Map.....	2-9
3-1	Power Turbine Simulator Test Rotor Schematic.....	3-3
3-2	Bearing Pedestal.....	3-4
3-3	Spring Support Cartridge.....	3-5
3-4	Spring Support Cartridge.....	3-6
3-5	Schematic of Cartridge Calibration Set-up.....	3-9
3-6	Typical Cartridge Calibration Curve.....	3-10
3-7	Assembled Test Rig.....	3-13
3-8	Test Rig Rotordynamic Model.....	3-16
3-9	Mode Shape Comparison - First Mode.....	3-17
3-10	Mode Shape Comparison - Second Mode.....	3-18
3-11	Test Rig Low Speed-Flexible Balancing Map.....	3-20
3-12	Test Rig Configuration I.....	3-24
3-13	Rig Configuration I Center Probe Response Balance at 2,500 RPM.....	3-25
3-14	Test Rig Configuration I Center Probe Response Balance at 5,000 RPM.....	3-26
3-15	Test Rig Configuration I Center Probe Response Balance at 7,500 RPM.....	3-27
3-16	Rig Configuration I Center Probe Response Balance at 8,000 RPM.....	3-28

LIST OF FIGURES (cont'd)

Figure		Page
3-17	Test Rig Configuration I Center Probe Response High Speed Balance (4,800 RPM and 16,000 RPM).....	3-29
3-18	Test Rig Configuration II.....	3-31
3-19	Test Rig Configuration II Titanium Disk Probe Response Balance at 8,000 RPM.....	3-33
3-20	Test Rig Configuration III.....	3-34
3-21	Test Rig Configuration III Center Probe Response Balance at 3,000 RPM.....	3-35
3-22	Test Rig Configuration III Center Probe Response Balance at 5,000 RPM.....	3-36
3-23	Test Rig Configuration III Center Probe Response Balance at 6,000 RPM.....	3-37
3-24	Test Rig Configuration I Center Probe Response Balance at 6,000 RPM.....	3-39
3-25	Test Rig Configuration I Center Probe Response Rigid Balance.....	3-40
4-1	NASA HPOTP Balance System.....	4-5
4-2	Balance System Software Block Diagram.....	4-8
4-3	Vibration Data Acquisition.....	4-10
4-4	Balance Sequence.....	4-11

LIST OF TABLES

Table		Page
3-1	Predict Spring Cartridge and Pedestal Stiffness.....	3-8
3-2	Cartridge Stiffness - Measured Versus Predicted.....	3-12
3-3	Summary of Test Configurations.....	3-23

1.0 INTRODUCTION

Under contract to NASA, Mechanical Technology, Inc. has developed a method for balancing rotors at low speed, which ensures smooth high-speed operation (i.e., operation above bending critical speeds). This method has been targeted for eventual hardware application to Space Shuttle Main Engine (SSME) pumps with particular attention given to the High Pressure Oxidizer Turbopump (HPOTP). The need for development of this low-speed flexible rotor balancing method arises from the fact that satisfactory operation of SSME turbopumps requires that shaft response amplitudes and forces transmitted through the bearings (to the housing) be minimized. Because rotor imbalance is a major cause of large amplitudes and high forces, it is necessary that these pumps be well balanced throughout their operating speed range.

In general, shaft response and transmitted force due to unbalance are greatest at or near critical speeds. The two SSME turbopumps, the HPOTP and the HPFTP, operate above their first bending critical speeds. Furthermore, the maximum operating speed for the HPOTP is above its second bending critical speed, and as the desired power level of the HPOTP is increased, its operating speed also approaches its second flexible critical speed. Thus, a method of balancing either rotor through two bending critical speeds is needed.

There are two general approaches to balancing rotating equipment: low-speed rigid and "high-speed" flexible methods. For the HPOTPs and HPFTPs, low-speed rigid balancing, by itself, is not adequate. In particular, correction weights predicted during rigid body balancing may worsen the state of balance at operating speed (i.e., resulting in increased rotor response and bearing forces) since the SSME turbopumps operate above flexible critical speeds. This leaves at speed flexible balancing of the SSME turbopumps as the only viable way to ensure smooth, balanced operation at high speeds. The ideal situation is to balance at critical and maximum operating speeds using a conventional multiplane, multi-speed flexible rotor balancing method. Furthermore, balancing should be performed in the actual housing, but out-of-housing balancing at critical and maximum operating speeds could be a satisfactory alternative if suspension characteristics are similar to those in the housing. However, these balancing approaches are impractical for the HPOTP for several reasons:

- Operating speeds are above one critical speed and approaching the second, yet only one plane is readily available for in-housing balancing of the assembled rotor

- Balancing speed is limited to 1500 rpm when performing in-housing balancing of the rotor since no coolant is available for the bearings during the balancing operation other than a liquid oxygen (LOX) compatible lubricant

- Bearing life is very short precluding a significant number of high-speed balancing runs regardless of a coolant/lubricant

- Bearing pairs are uniquely matched to each rotor, thereby preventing approaches where sacrificial bearings might be used during an out-of-housing assembled rotor-balancing procedure

- Excessive bearing loads that limit the already short life must be minimized

- Only LOX-compatible substances can be used to cool and lubricate the bearings to avoid system contamination if speeds higher than those currently used are anticipated

- Rotor vibration data are extremely difficult to record from in-housing operation since only case-mounted accelerometers are currently used.

As a result of these hardware constraints, neither in-housing nor out-of-housing, high-speed, flexible balancing can be used on SSME turbopumps.

Despite the difficulties, a method has been developed that shows promise in overcoming many of these limitations. This method establishes one or more "windows" for low-speed, out-of-housing balancing of flexible rotors. These windows are regions of speed and support flexibility where two conditions are simultaneously fulfilled. First, the rotor system behaves flexibly: therefore, there is separation among balance planes. Second, the response due to balance weights is large enough to reliably measure.

This report describes the analytic formulation of the low-speed flexible rotor balancing method. In addition, the results of proof-of-principle tests conducted under the program are presented. Based on this effort, it is concluded that low-speed flexible rotor balancing is a viable technology. In particular, the method can be used to balance a rotor bearing system at low speed which results in smooth operation above more than one bending critical speed. Furthermore, this balancing methodology is applicable to SSME turbopump rotors.

2.0 LOW-SPEED FLEXIBLE ROTOR BALANCING

The objective of developing a low-speed flexible rotor balancing methodology under this program is to overcome limitations that low-speed rigid and high-speed flexible balancing methods present when applied to SSME turbopumps. Specifically, the developed approach eliminates the need for high-speed balance runs, but nonetheless reduces rotor response to unbalance during high-speed operation.

2.1 Formulation

The objective of rotor balancing methods is to predict weights to be added (or removed) from a rotor-bearing system to minimize unbalance response. That is, weight distributions are predicted which, ideally, produce amplitudes at measurement planes equal to those resulting from rotor unbalance, only 180 degrees out of phase. The vector sum of response at those measurement planes is therefore nil, at the balancing speed(s), but this may not be the case at other speeds. With the low-speed flexible rotor balancing method, weights are predicted at a low speed(s) for balance planes located at the major sources of potential unbalance, such that response is minimized at both the balancing speeds and also at higher speeds (i.e., the operating speed).

To perform low-speed flexible balancing, the following steps are required:

- Select the required balance planes
- Determine speeds at which there is separation among the selected balance planes (i.e., is the rotor sufficiently flexible?)
- Determine speeds at which the rotor response is acceptable (i.e., is the response measurable with sufficient accuracy?)
- Perform influence coefficient balancing where the rotor is both flexible and responsive.

Balance plane selection is based on several considerations. First, only balance planes which are compatible with actual hardware can be used (i.e., axial planes where weight can be added or removed at any circumferential location). Second, balance planes which are active (i.e., not at nodes) at the speeds of interest and at the maximum operating speed of the equipment should be used. Finally, the balance planes must be active at the speed(s) where low-speed balancing will be performed. This last condition is, to some extent, controllable by proper configuration of the balancing hardware (in particular, by proper selection of bearing support flexibilities). In all cases, engineering judgment is required to select the proper balance planes to be used with the balancing method.

After balance planes have been selected, the next step in the low-speed flexible balancing method is to determine plane separation. One obvious case of when balance planes are not separated occurs when they are in close proximity to one another. In this case, a weight in either plane causes the same rotor response.

In general, however, plane separation depends on the rotational speed of the shaft and flexibility of the rotor supports (i.e., bearing supports to ground). The following three cases, which depend on rotational speed and support flexibility, are possible:

- There is only one required plane at any critical speed since (at these speeds) the entire rotor vibration is controlled by any one active imbalance on the rotor.

- At off-critical speeds where the supports are flexible (as compared to the rotor), the rotor behaves as a rigid body and two balance planes are necessary. At these speeds, the rotor can be balanced by counteracting the forces and moments due to unbalance. Two balance planes provide the required two degrees of freedom.

- At off-critical speeds where the rotor is flexible, plane separation exists for all balance planes (other than those in close proximity to one another).

These regimes are shown schematically in Figure 2-1.

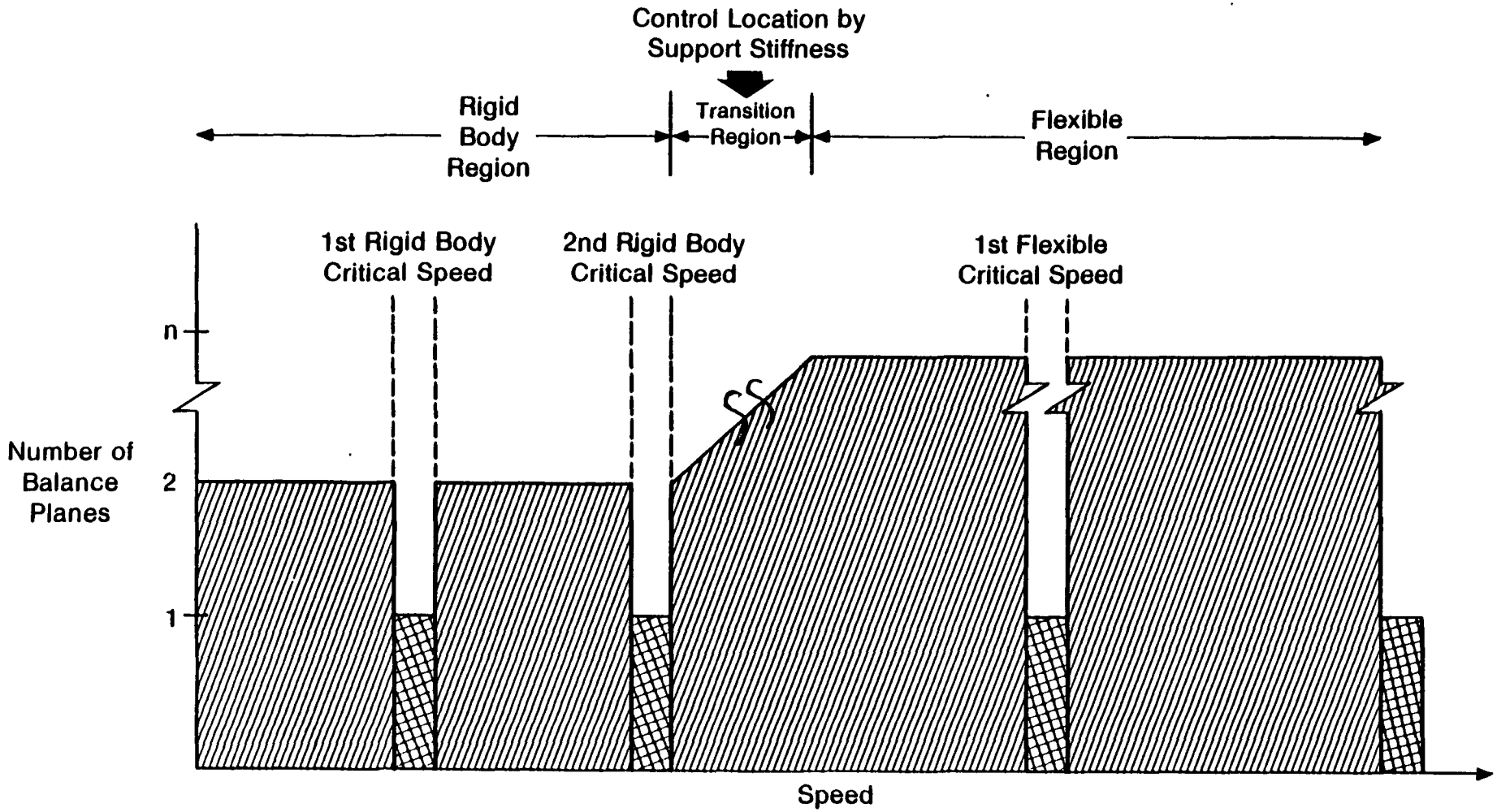

Figure 2-1 Required Number of Balance

One approach for determing plane separation uses the influence coefficient matrix. With this approach, separation among selected balance planes can be assessed for different support flexibilities and speeds. Regions of expected plane separation are then mapped out as a function of support flexibility and speed.

In addition to locating plane separation regimes, it is necessary to determine the expected levels of rotor response. This is particularly important because low-speed flexible rotor balancing will be performed at off-critical speeds where response is usually small. "Responsiveness" needs to be assessed so as to determine when expected response is large enough to measure and to select probes that have the desired resolution. Responsiveness of the rotor at the speeds being considered for balancing can be assessed by performing a forced response rotordynamics calculation. This is done by including a distributed unbalance in a rotordynamics model of the rotor-bearing system. To ensure that the magnitude and phase of the unbalance(s) used in the calculation are realistic, they should first be used to calculate response at speeds where measured response data are known. For example, if response at maximum operating speed is known, the magnitude and phase of the distributed unbalance can be adjusted until the predicted response is similar to measured response. Then, when this unbalance is used to predict response at the balance speeds, it will yield an indication of expected response at these speeds. These results are used to select the required instrumentation sensitivity, or, conversely, to rule out ranges where responsiveness is too small to be accurately measured.

The purpose of this balancing method is to determine the lowest speed at which balancing can be performed where the rotor is flexible. The approach previously described is used to determine the parameters needed for successful low-speed balancing: that is, required balance planes, plane separation regimes and instrumentation sensitivity requirements. Actual balancing is performed in regimes where plane separation exists and response can be measured using a multiplane influence coefficient balance method at the balance speed determined with these results.

2.2 HPOTP Low-Speed Flexible Balancing Assessment

The low-speed flexible rotor balancing method described in the previous section has been applied analytically to the HPOTP. This assessment was made to determine the overall feasibility of applying the low-speed flexible balancing method to this pump. The evaluation method consisted of the following:

1. Balance plane selection

2. Determination of plane separation

3. Determination of responsiveness

Balance plane selection was based on a review of HPOTP drawings and design information provided to MTI. Based on this review, available balance planes were identified as shown in Figure 2-2. From this set of available planes, three planes were selected for use with Step 2 above. The major criterion used for selecting these three planes was that they be active in the modes within the operating speed range of the HPOTP in its in-housing configuration. The HPOTP has one critical speed below its current maximum speed and a second near the maximum speed at increased power levels. The mode shapes for these two critical speeds are shown in Figure 2-3. Figure 2-2 shows the model used for rotordynamic calculations (i.e. critical speeds, mode shapes, influence coefficients, and response). Based on the available planes and the critical speed mode shapes, three balance planes were selected for determination of plane separation: main impeller, preburner impeller and first stage turbine end.

As stated earlier, one objective of the low-speed flexible balancing method is to determine the lowest speed at which the selected balance planes are separated. Plane separation generally depends on the rotational speed of the shaft and the flexibility of the rotor supports (i.e., bearings to ground). An assessment of plane separation for different values of speed and support flexibility for the HPOTP was made using a model of the HPOTP. Influence coefficient matrices using these three planes were calculated for rotational speeds below 10,000 rpm and selected ranges of support flexibility. The influence coeffi-

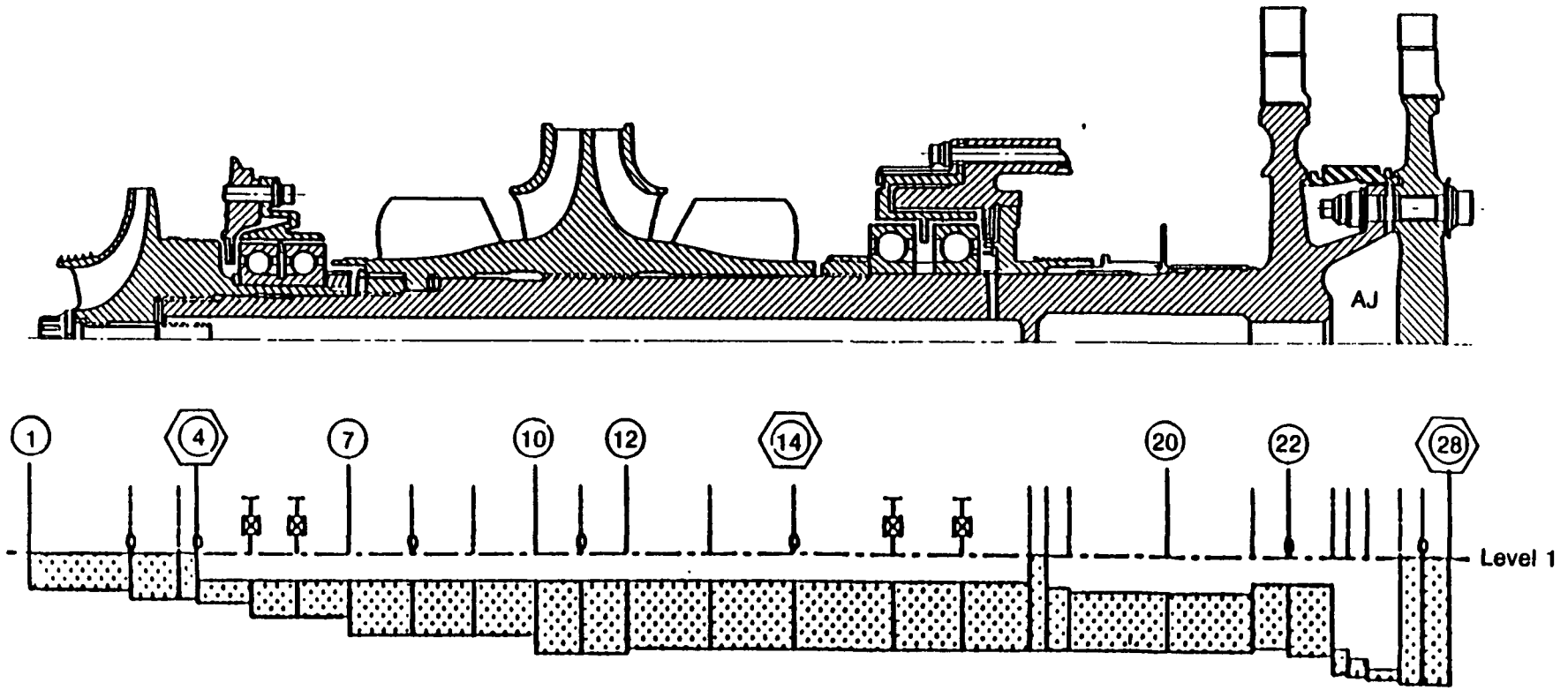

Figure 2-2 HPOTP Balance Planes

83778-3

HPOTP ROTOR

Mode Number 1: 11,537 rpm

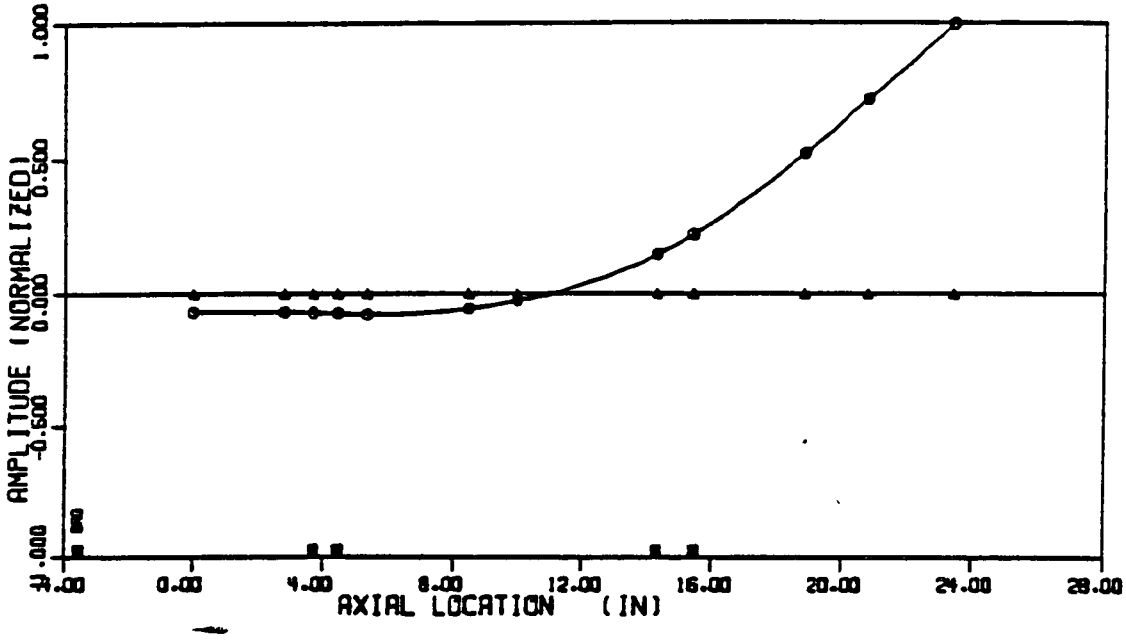

HPOTP ROTOR

Mode Number 2: 36,082 rpm

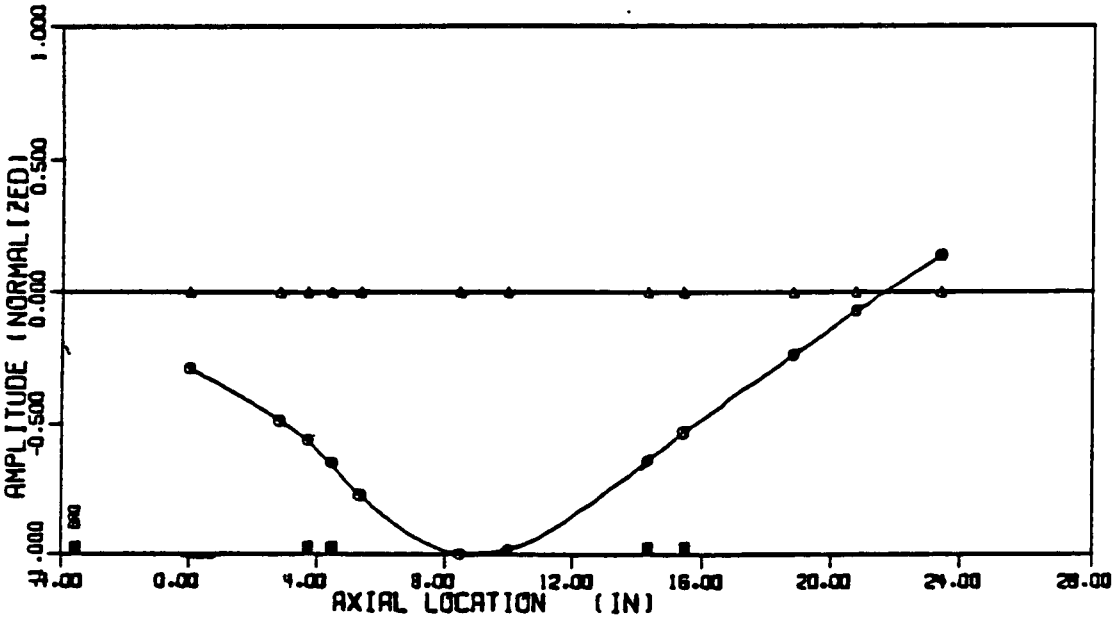

Figure 2-3 HPOTP Mode Shapes

cient matrices were used to determine speeds at which the HPOTP behaves in a flexible manner for each value of support flexibility considered.

In addition to plane separation, HPOTP response to unbalance was assessed to determine "responsive" regimes. This was accomplished by performing a response calculation with a randomly distributed unbalance. An unbalance distribution which caused a response of approximately 1 G at the bearings (at 30,000 rpm) was used. This level of unbalance was selected since it nominally represents the amount of unbalance seen in the HPOTP. This same distributed unbalance was used to predict response at lower speeds with the support flexibilities used for the plane separation assessment. To use these results, it was assumed that response of 0.05 mils could be accurately measured (this is the resolution of a capacitance probe system for this application). Thus, at speeds where response is greater than 0.05 mils, the HPOTP was considered to have measurable response (i.e., it is "responsive").

For this HPOTP analysis, Figure 2-4 shows the regions where plane separation occurs and the rotor is responsive, for different values of speed and support flexibility. The regimes where these two conditions occur simultaneously are the low-speed flexible rotor balance regimes. As shown in the figure, for a support flexibility of 1,000 lbs./in., balancing could be performed as low as 6,000 rpm. As flexibility is decreased, the speed at which successful balancing is predicted decreases. In particular, for support stiffness values between 10,000 lbs./in. and 100,000 lbs./in., there are "windows" between the first and second mode where low-speed flexible balancing regimes are predicted. These occur where plane separation and rotor responsiveness coincide. The lowest predicted balance speed in these regions is approximately 3,000 rpm and is for a support stiffness of 10,000 lbs./in.

In Figure 2-4, it is interesting to note that for support stiffnesses of 50,000 lbs./in. and 100,000 lbs./in., plane separation is predicted at very low speeds. However, this figure also shows that for these speeds, predicted response is below the measureable regime. This demonstrates that instrumentation sensitivity may be a key parameter in this low-speed flexible balancing method. In particular, lower balance speeds will be predicted for instrumentation with greater sensitivity.

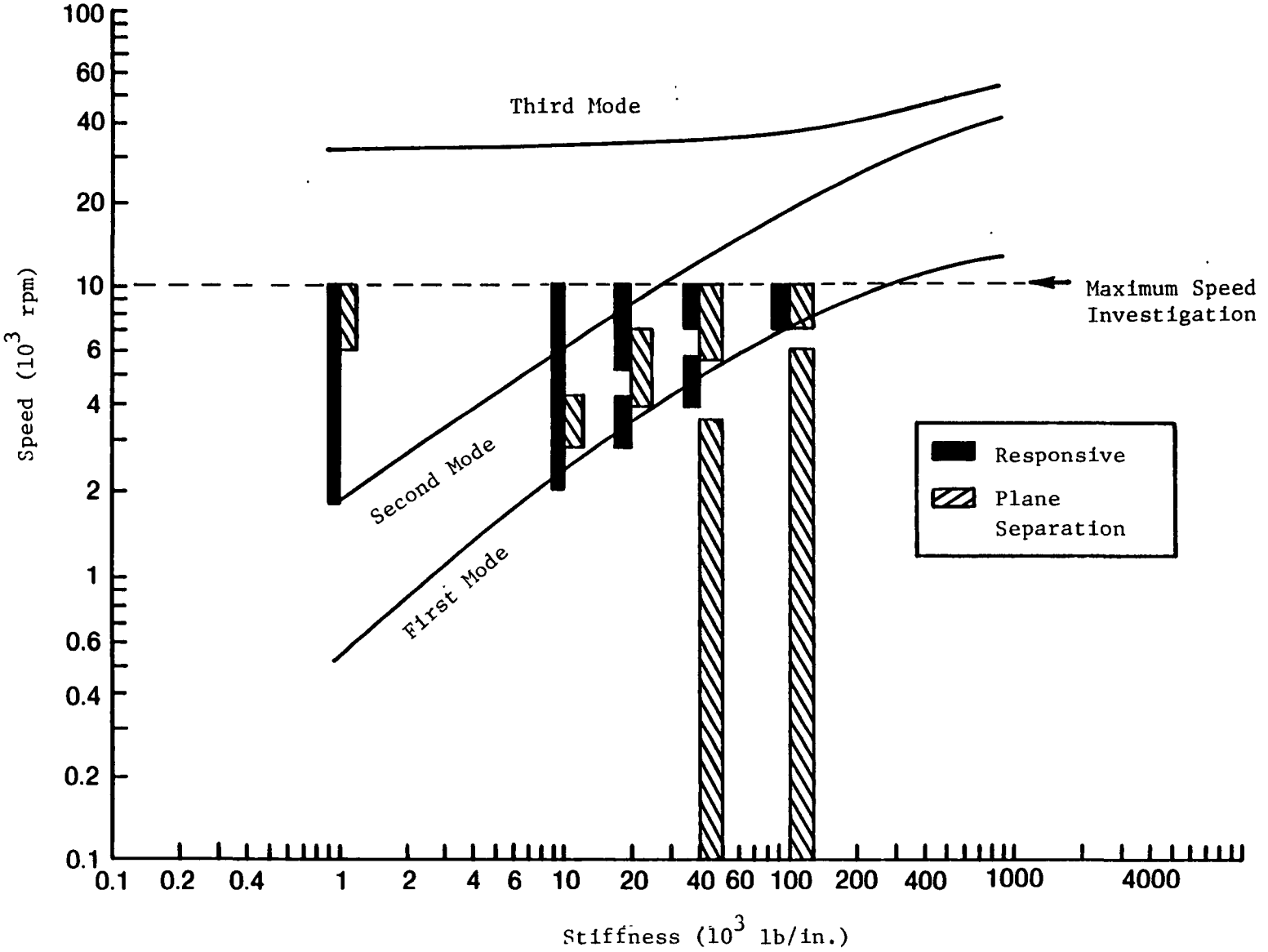

Figure 2-4 HPOTP Low-Speed Flexible Balancing Map

85609

In summary, a method for predicting low-speed flexible balance regimes has been developed. This method predicts "windows" of support flexibility and speed where a rotor exhibits plane separation and where response can be reliably measured. Furthermore, this method has been applied to an HPTOP rotor model and balance speeds as low as 3,000 rpm have been predicted.

3.0 EMPIRICAL EVALUATION

An empirical evaluation of the flexible rotor balancing method was conducted using a rotordynamic test rig. The objective of this proof-of-principle testing was to determine the effectiveness of low-speed flexible rotor balancing in a controlled laboratory environment. Furthermore, test hardware and test conditions were selected based on the fact that the eventual application of the method is for the HPOTP.

To perform the empirical evaluation, it was necessary to use a suitable test rig. A set of criteria were established so that various in-house rigs could be evaluated for this use. For example, since the rig was to be used to determine the effectiveness of the low-speed flexible rotor balancing method for smooth supercritical operation, it needed to have bending criticals below its maximum speed. Furthermore, since the eventual application of the method is for the HPOTP, similarity between the test rig mode shapes and the HPOTP mode shapes was considered to be an important criterion. As described in Section 2, the low-speed flexible balancing method is based on finding plane separation regimes for different values of support stiffness. Thus, it was necessary to have a rig whose bearing support stiffness could be varied. In summary, the test rig selection criteria were as follows:

- Bending critical speeds within the operating speed range
- Mode shapes similar to the HPOTP
- Ease of incorporation of variable support flexibility

Initially, a cursory assesment of several rigs was made and compared to the above criteria. The results of this assessment showed that one of these rigs was particularly suitable for this test effort. This rig was further analyzed and subsequently was selected for empirical evaluation. The remainder of this section describes the test rig, analysis and test results.

3.1 Test Rig Description

The rig which was selected for the empirical evaluation test was orginally designed to simulate the power turbine of a gas turbine engine and included:

- Flexible shaft with an integral drive turbine and overhung disk
- Maximum speed of 24,000 rpm
- Two pairs of duplex ball bearings for shaft support
- Bearing pedestals with interchangeable supports

A schematic of the test rig shaft assembly is shown in Figure 3-1. This assembly consists of a slender shaft with a disk attached to each end. Both of these disks were originally designed to simulate inertias on the original power turbine. One of the disks also serves as a drive turbine. Both of these disks were also used as balance planes. For insertion of balance weights, the drive turbine disk has 24 axial holes on a 2.5 inch diameter, and the larger titanium disk has 36 axial holes on a 9.5 inch diameter. A maximum of about 1 gram can be installed in each of the holes. There are two additional balance planes, both along the slender shaft which are integral rings with 12 flats. Each flat has a radial hole for insertion of a balance weight. The maximum amount of weight which could be installed in each hole of these center balance planes is also 1 gram.

The shaft assembly is supported on two duplex pairs of rolling element bearings and their locations are shown in Figure 3-1. A schematic of the bearing support pedestals is shown in Figure 3-2. The pedestals provide lubrication and cooling oil supply/drain, and were originally designed to accept interchangeable cartridges with elastomer supports. For this balancing evaluation, elastomer supports were not considered acceptable since they generally introduce substantial external damping to the rotor-bearing system. However, the pedestals were ideal for use in the current test program since support flexibility could be easily changed by a redesign of the cartridges.

The redesigned support cartridges used for the balancing evaluation are shown schemetically in Figure 3-3. As seen in this figure, the cartridges were designed to accept spring washers so that different sized washers (i.e., wavy or belleville) could be used to achieve different support flexibilities. A photograph of a cartridge during the assembly process is shown in Figure 3-4. The design values for support flexibility were selected using the results of the low-speed balancing assesment which is discussed in Section 3.2. In particular,

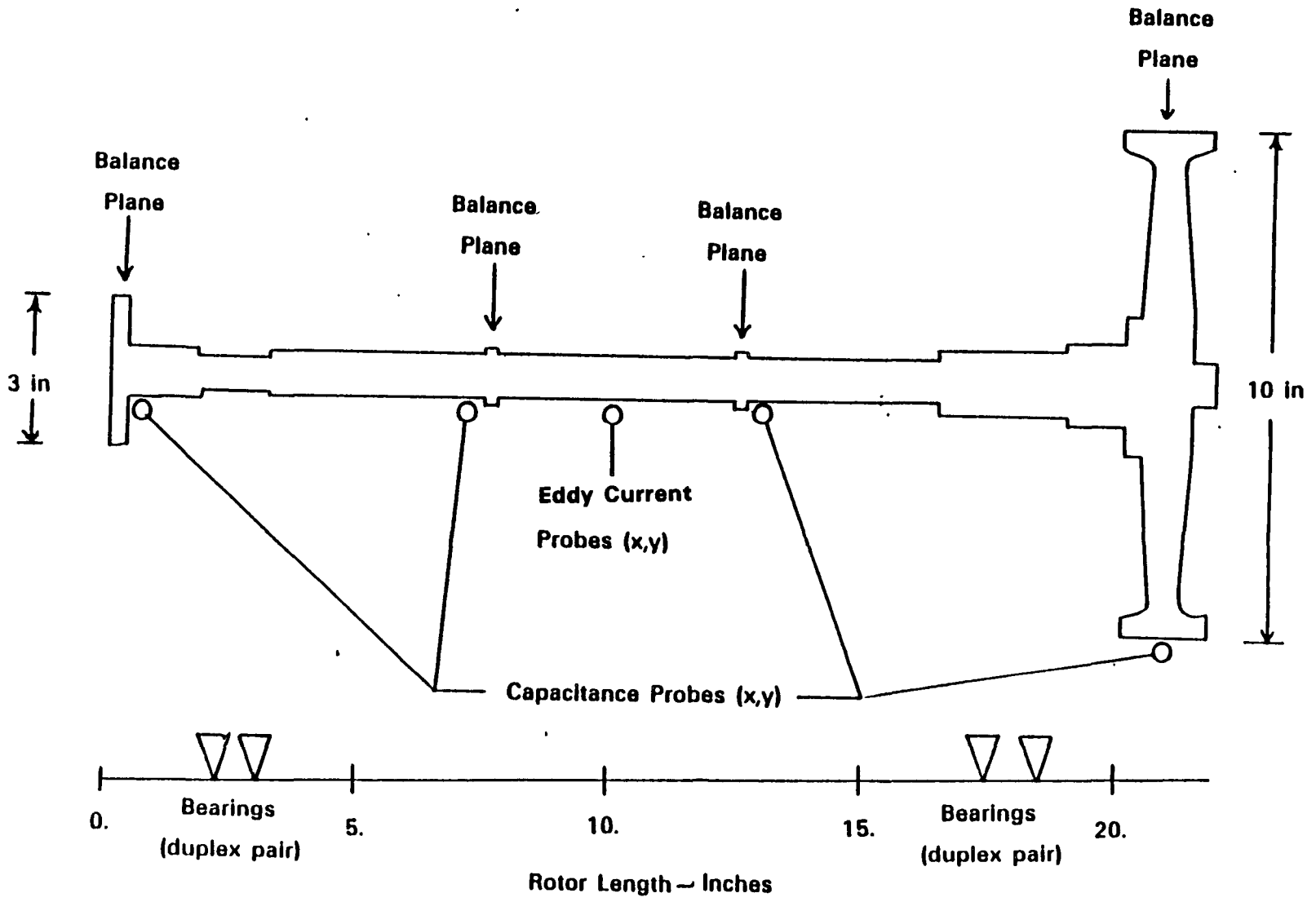

Figure 3-1 Power Turbine Simulator Test Rotor Schematic

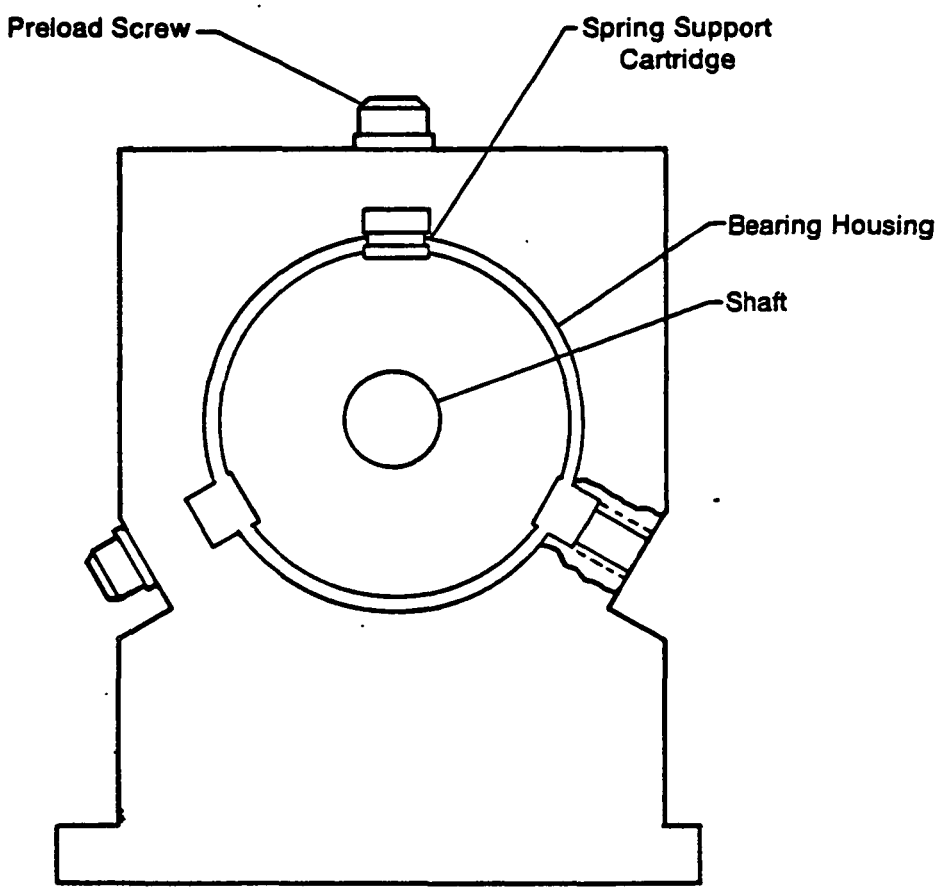

Figure 3-2 Bearing Pedestal

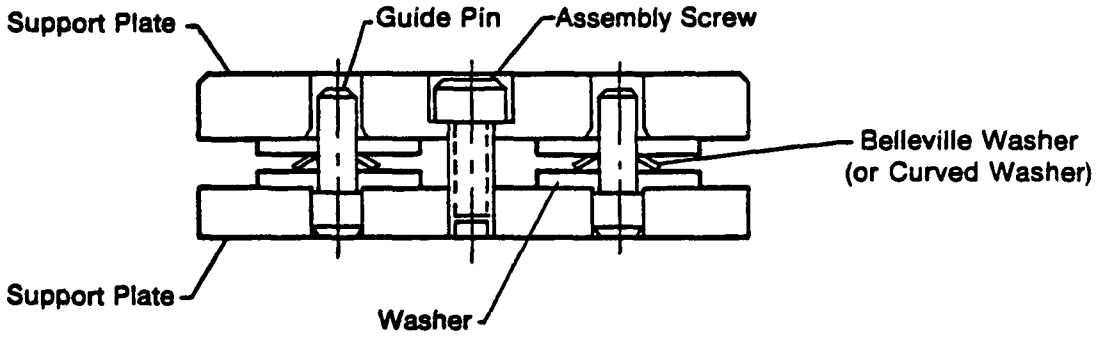

Figure 3-3 Spring Support Cartridge

Figure 3-4 Spring Support Cartridge

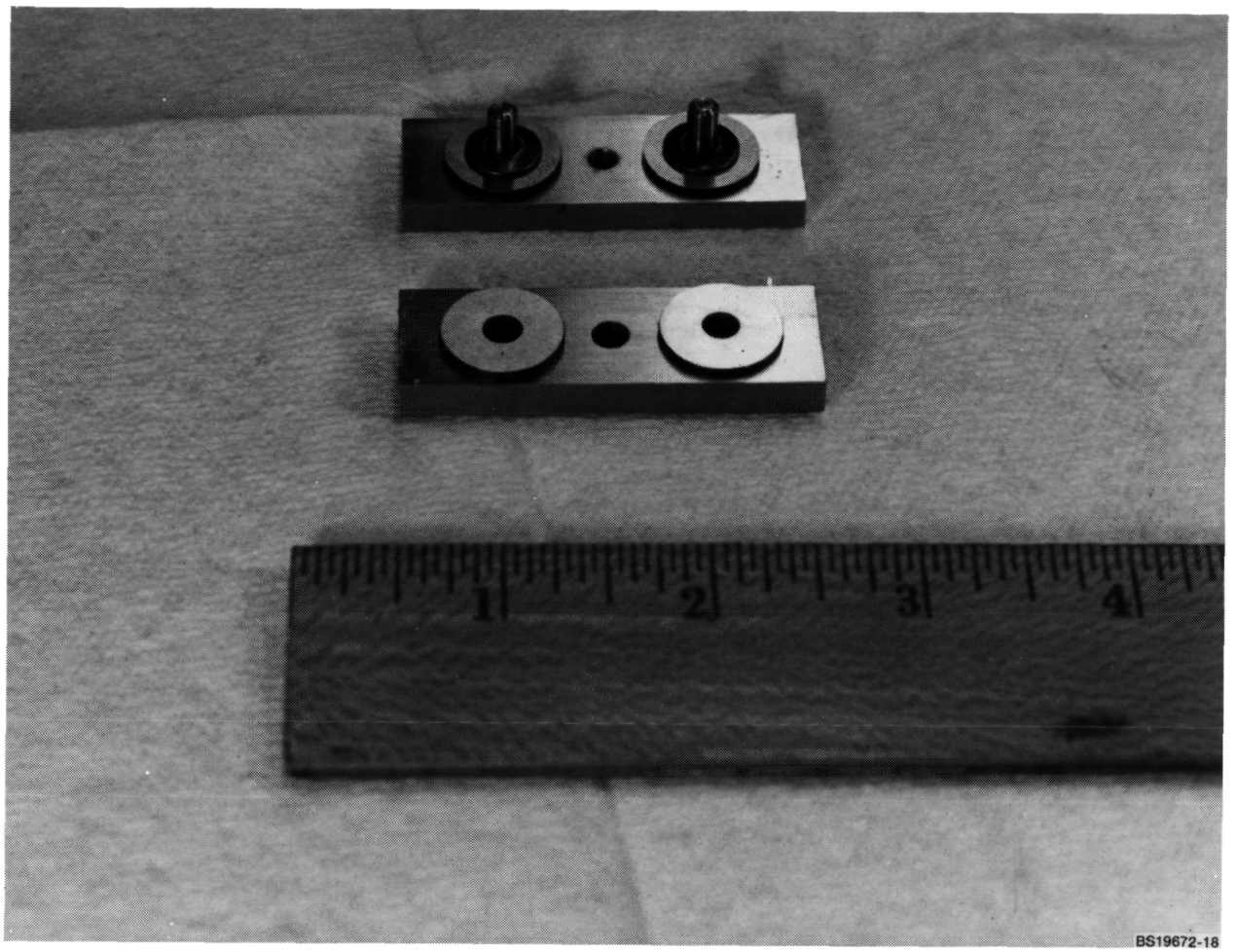
1
2
3
4
BS19672-18

pedestal support flexibilities of 2, 4, 20, and 100 thousand lbs./in. were required.

To design for the desired support stiffness values, a method for predicting total stiffness based on individual washer stiffness was established. In particular, the stiffness of each cartridge is twice the individual washer stiffness since these are parallel springs. From Ref. [1] the stiffness of the bearing pedestal assembly, which consists of three cartridges 120° apart, is equal to 1.5 times the cartridge stiffness. This assumes that the cartridge has radial stiffness only and no shear (i.e., tangential) stiffness. This is a valid assumption since the cartridges offer no significant resistance to tangential forces. In summary, the total pedestal stiffness k_t is:

$$k_t = 3 \times k_w$$

where k_w is the washer stiffness.

To achieve the desired pedestal assembly stiffness, different sizes and types of commercially available washers were assessed. Stiffness values, (or equations for calculating stiffness), were obtained from manufacturers' specifications for these washers. Table 3-1 summarizes calculated stiffness for the washers used in the cartridge.

To verify the stiffness values shown in Table 3-1, the cartridges were calibrated. Calibrations were performed on the cartridge assembly (not the individual washers) shown in Figure 3-3. The calibration set up is shown in Figure 3-5. The procedure consisted of applying a compressive load through the center of the cartridge assembly and measuring applied force and displacement. Force and displacement measurements were made for increasing and decreasing load, so that hysteresis could be qualitatively assessed. The maximum force used for calibrating each cartridge assembly was based on manufacturers' specifications.

A typical force vs. displacement curve obtained during calibration is shown in Figure 3-6. The assembly is seen to be nearly linear over the load range and the amount of hysteresis is not significant. For each cartridge/washer assembly, the stiffness was determined by taking the slope of the force vs. displacement curve. In addition, the force vs. displacement curve was used to determine how

TABLE 3-1

PREDICT SPRING CARTRIDGE AND PEDESTAL STIFFNESS

Spring No.	Washer Stiffness (lbs./in)	Cartridge Assembly Stiffness (lbs/in)	Pedestal Assembly Stiffness (lbs/in)
1	600	1200	1800
2	1167	2333	3500
3	7733	15466	23200
4	33438	66876	100314

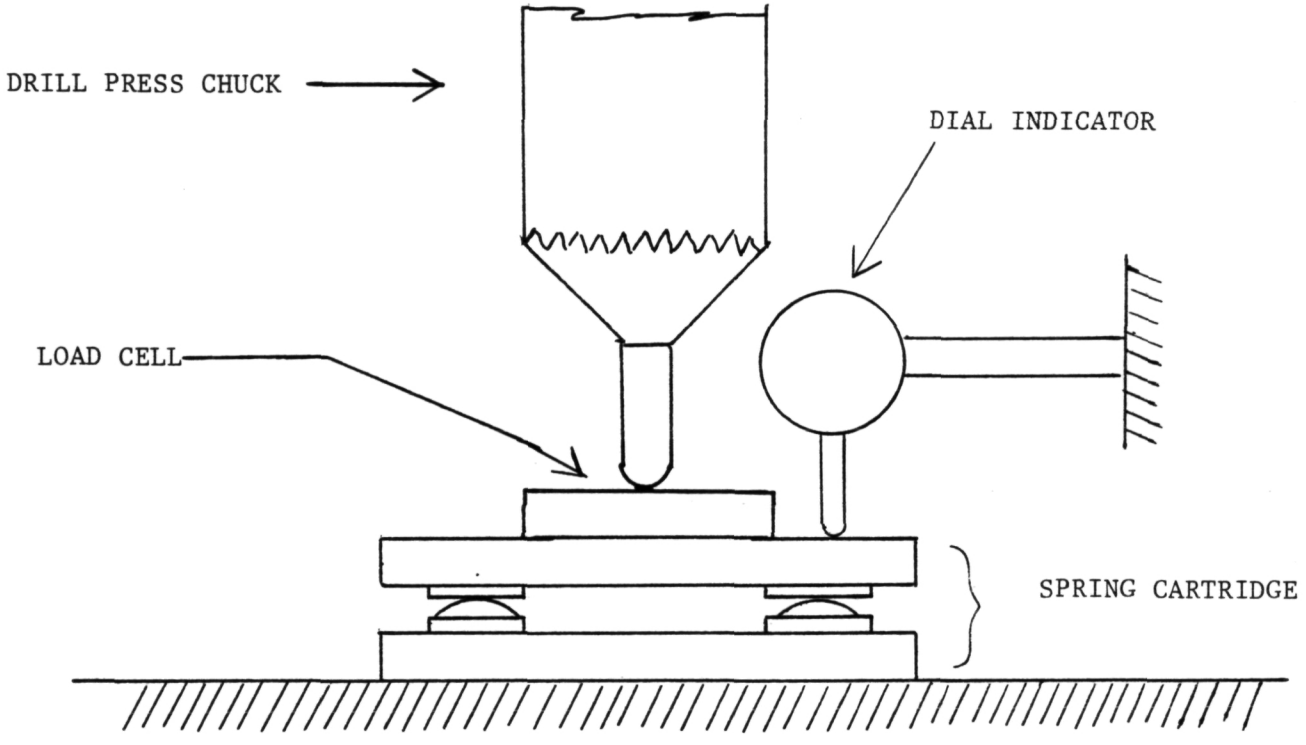

Figure 3-5 Schematic of Cartridge Calibration Set-up

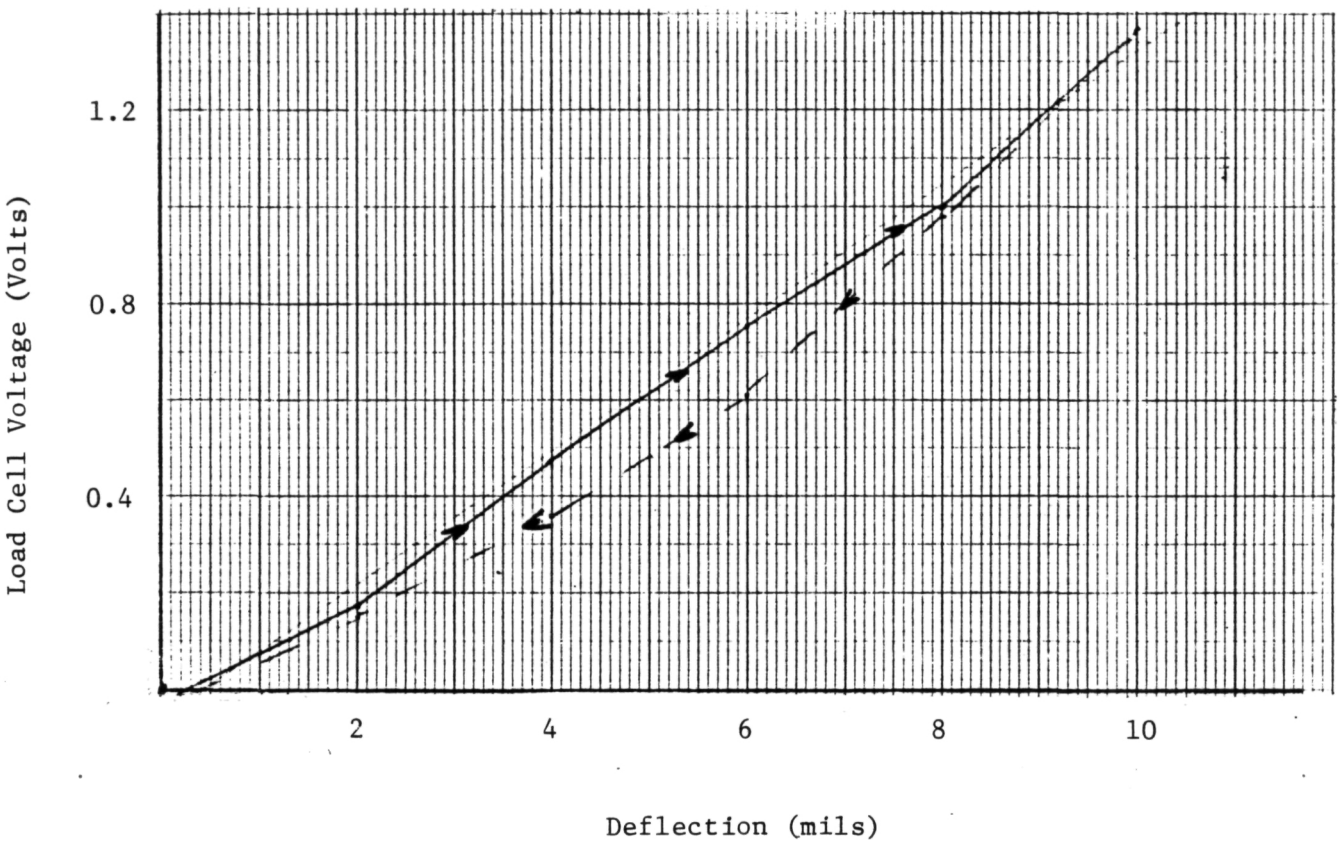

Sample Cartridge Stiffness Calculation

$$K = \frac{\Delta \text{ Force}}{\Delta \text{ Deflection}} = \frac{\Delta V}{\Delta X} \times \text{calibration factor}$$

$$K = \frac{1.32 - (-0.06)}{0.010} \times 100 = 13{,}800 \text{ lbs/in}$$

Figure 3-6 Typical Cartridge Calibration Curve

much preload to apply to each cartridge/washer assembly when installed in the bearing pedestals. In particular, the preload (in mils) was selected as the deflection at the midpoint of the linear range. Table 3-2 is a summary of the measured cartridge displacement as compared to the predicted stiffness. These results show that the predicted and measured values of cartridge stiffness are in reasonable agreement.

The test rig was instrumented with a series of capacitance and eddy current measurement probes. The probe locations are shown in Figure 3-1. The capacitance probes were used for balancing since they provide greater accuracy than the eddy current probes. Their locations were selected based on the balancing assesment discussed in Section 3-2. The eddy current probes were used for initial debugging and for monitoring rig response during high-speed operation. In particular, the latter probes were installed with a probe/shaft gap of approximately 15 mils and, therefore, there was less risk of damage should large shaft orbits be encountered. On the other hand, the capacitance systems required a probe/shaft gap of approximately 6 mils. This gap requirement was not a limitation during actual balance runs since amplitudes were typically on the order of 3 mils.

In summary, the selected test rig was modified to include variable support stiffness and instrumented with probes for balancing and for monitoring high-speed operation. Figure 3-7 is a photograph of the assembled rig. The following section describes the rotordynamics and balancing assesment of the test rig.

3.2 Test Rig Analysis

A rotordynamic model of the test rig was prepared so that the rig system could be analyzed. Initially, the rig was analyzed to determine its critical speeds. Next, the low-speed flexible balance regimes were calculated using the method discussed in Section 2.

TABLE 3-2

CARTRIDGE STIFFNESS - MEASURED VERSUS PREDICTED

Spring Number	Predicted Cartridge Assembly Stiffness (lbs/in)	Measured Cartridge Assembly Stiffness (lbs/in)
1	1200	1100
2	2333	2083
3	15466	13800
4	66876	85000

Figure 3-7 Assembled Test Rig

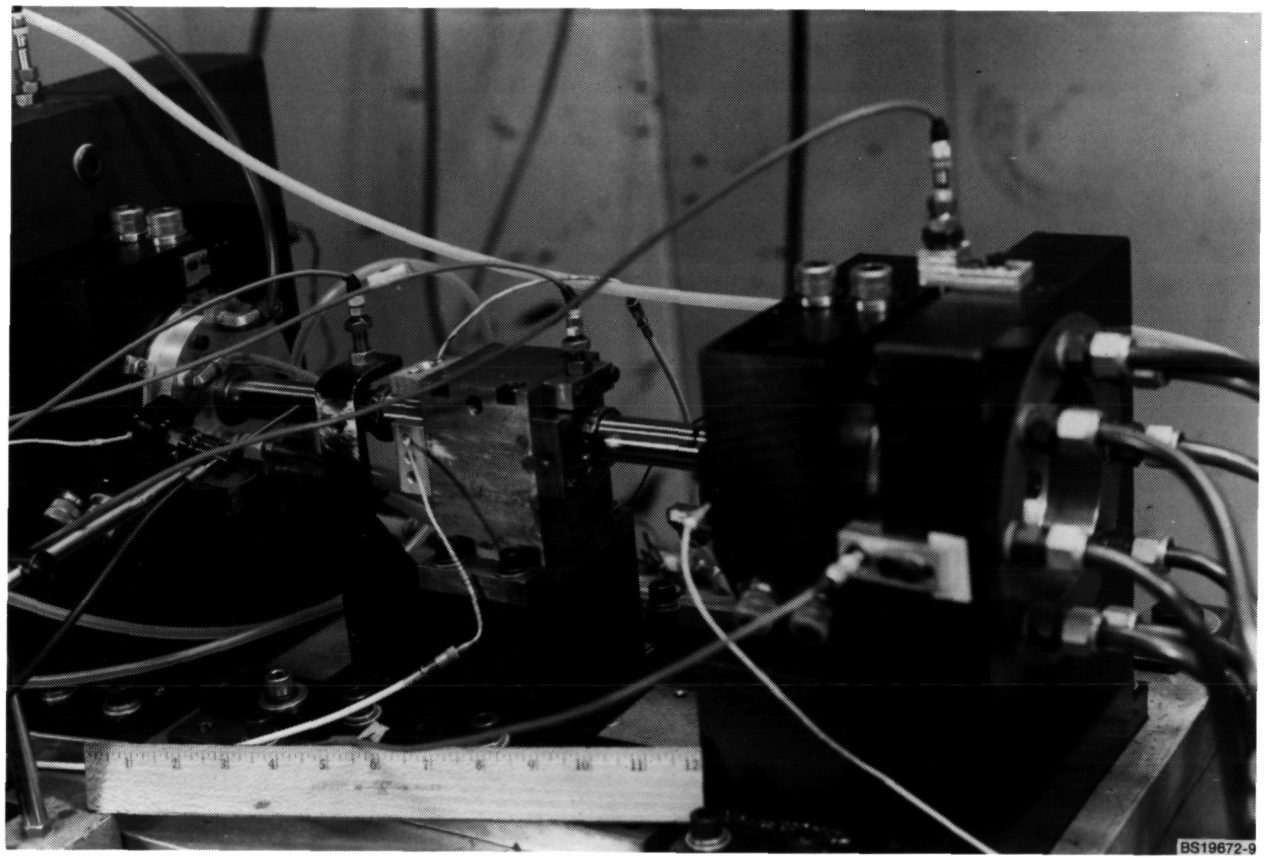
BS19672-9

The test rig was modeled so that it could be analyzed with PERFECT - MTI's finite element rotordynamic analysis computer program. The model is comprised of a three level system:

- Level 1 - Shaft and disk attachments
- Level 2 - Nonrotating components between the shaft and pedestal support cartridge on the drive turbine end
- Level 3 - Nonrotating components between the shaft and pedestal support cartridge on the titanium disk end

Each level is a mass/elastic model of the appropriate hardware components and takes into account geometry and material properties. In addition to the mass/elastic model of each level, there are several interlevel connections. Following is a summary of these interlevel connections:

- Level 1 to 2 - ball bearings between the shaft and the turbine end nonrotating components (modelled as two springs, one for each of the duplex pair)
- Level 1 to 3 - ball bearings between the shaft and the disk end nonrotating components (modelled as two springs, one for each of the duplex pair)
- Level 2 to Ground - flexibility of the spring support cartridge on the turbine end pedestal (modelled as two springs, one for each of the wavy washers in the assembly - each spring has one half the stiffness of the pedestal assembly)
- Level 3 to Ground - flexibility of the spring support cartridge on the disk end pedestal (modelled as two springs, one for each of the wavy washers in the assembly - each spring has one half the stiffness of the pedestal assembly)

The spring support cartridge models were based on nominal stiffness values. The ball bearings were modelled as infinitely stiff. This provided the best correlation with measured critical speeds.

A sample critical speed run is provided in Appendix A, and includes a tabular listing of the rotordynamic model. A graphic representation of the model is shown in Figure 3-8. The sample run in Appendix A represents the test rig configuration with supports selected to match the HPOTP critical speed mode shapes. Figures 3-9 and 3-10 show the predicted first and second critical speed mode shapes for the HPOTP and for the test rig (upper and lower plots in each figure, respectively). These figures show that the mode shapes for the test rig are similar to those of the HPOTP - the first mode being a "disk bounce" mode, and the second a bending mode. In addition, measured test rig mode shape data points are added to the lower plot on each figure. Mode shape measurements were made at the speeds indicated by using the capacitance displacement probes. The measured data were normalized and added to the predicted mode shape plots. There is good agreement between the measured and predicted shapes for the first mode, and excellent agreement for the second mode.

The calibrated rotordynamic model of the test rig described above was analyzed for application of the low-speed flexible rotor using the method discussed in Section 2. In particular, rotor responsiveness and plane separation of the rig were assessed for different speed and support flexibility ranges. Support flexibility was varied by using different values for the stiffness of the connections which represent the spring support cartridges.

To determine the rotor responsiveness, forced response calculations were performed by including a distributed unbalance in Level 1. The distributed unbalance was used to model forces caused by eccentricity of the balance planes. In addition, a small amount (1 lb.-sec./in.) of damping was included at each of the support ball bearings. A response greater than 0.5 mils at the capacitance probe locations was considered "measureable". This value of response was the expected resolution of the probes used on this rig.

Plane separation was also assessed using the rotordynamic model. As discussed in detail in Section 2, plane separation is assessed by using analytically predicted influence coefficients. Influence coefficients were calculated over the rig's speed and support flexibility range, and were used to determine plane separation.

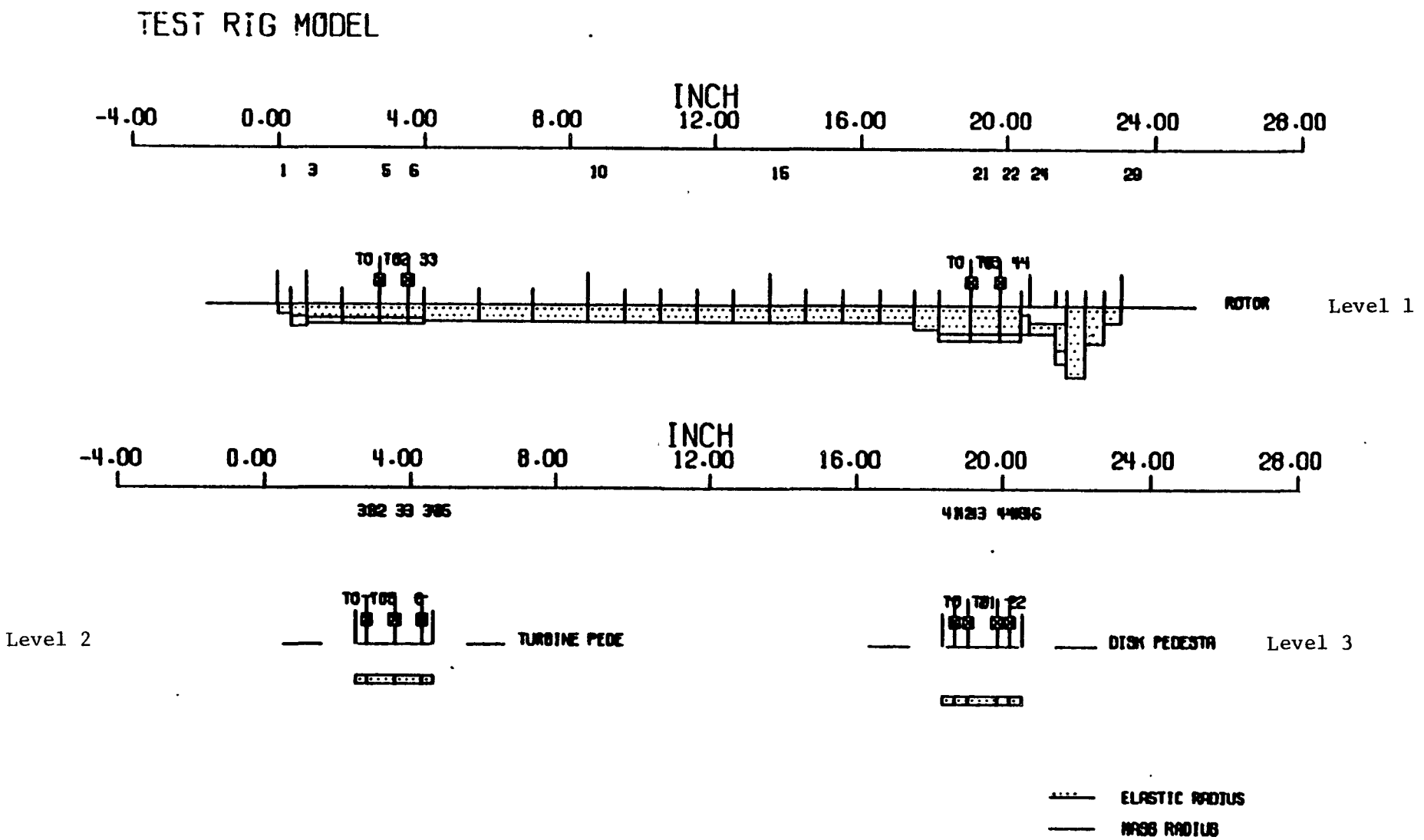

Figure 3-8 Test Rig Rotordynamic Model

HPOTP ROTOR

Mode Number 1: 11,537 rpm

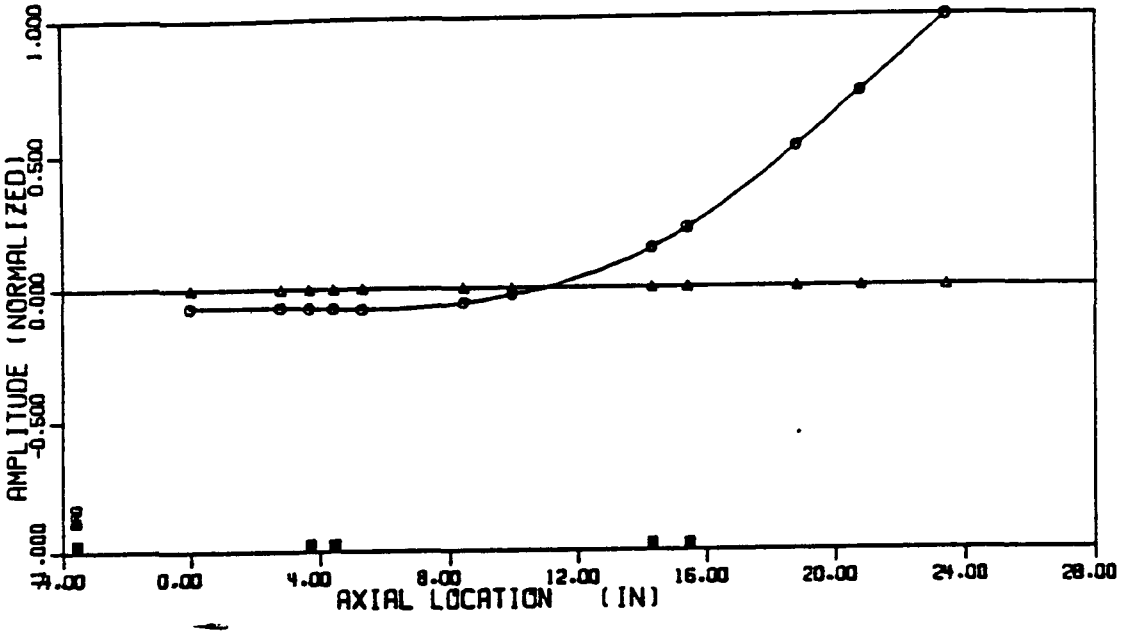

TEST RIG ROTOR

Mode Number 1: 4,967 rpm

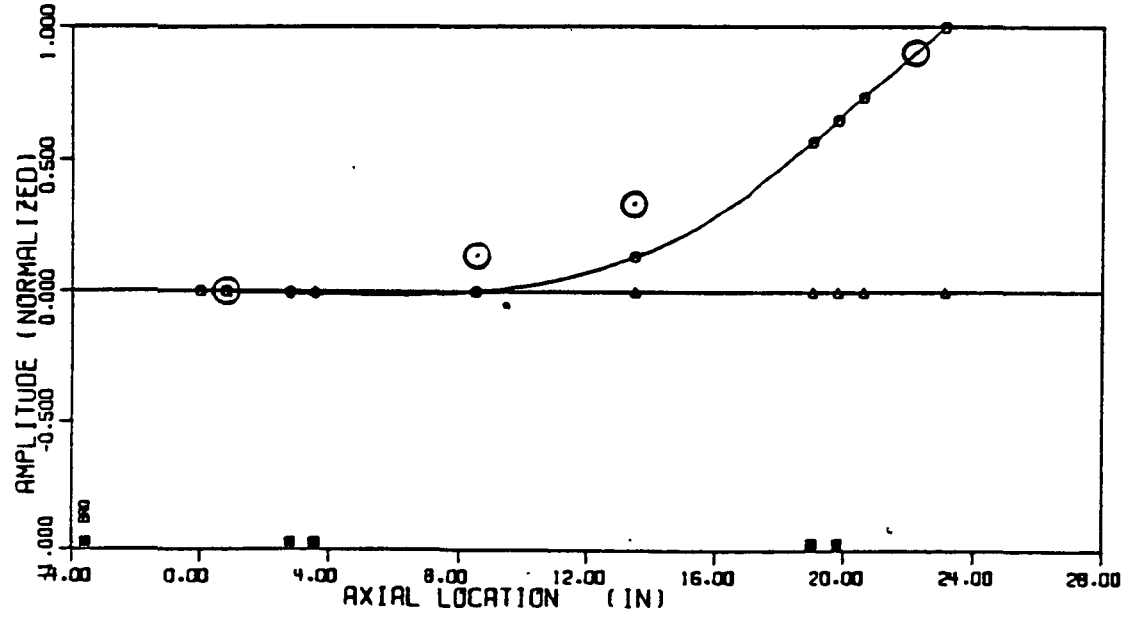

⊙ Measured at 4,700 rpm

85632

Figure 3-9 Mode Shape Comparison - First Mode

HPOTP ROTOR

Mode Number 2: 36,082 rpm

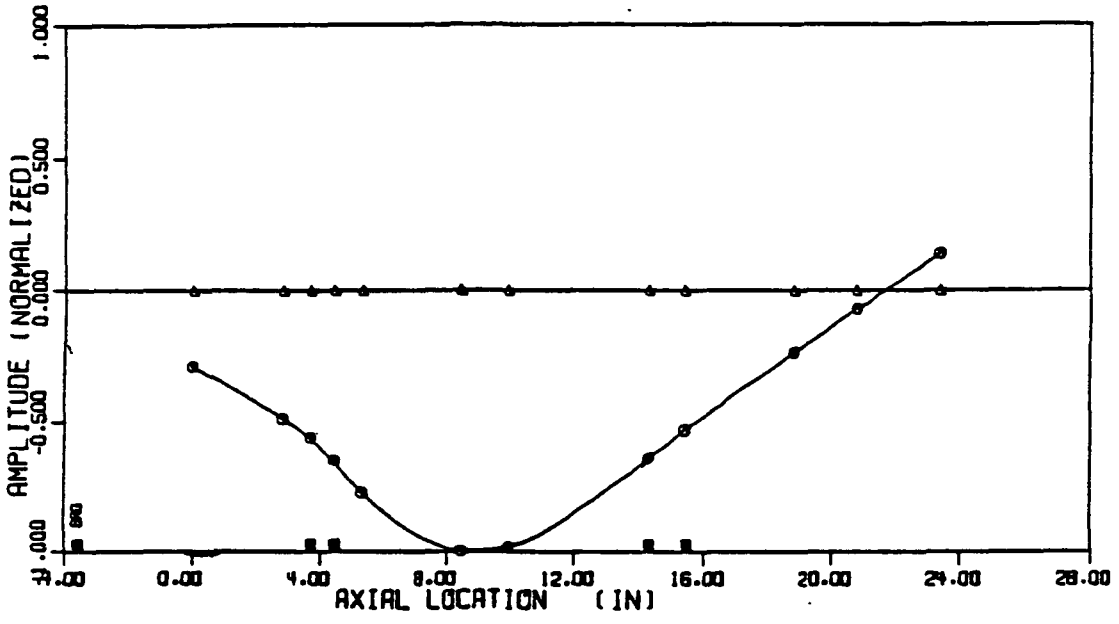

TEST RIG ROTOR

Mode Number 2: 23,550 rpm

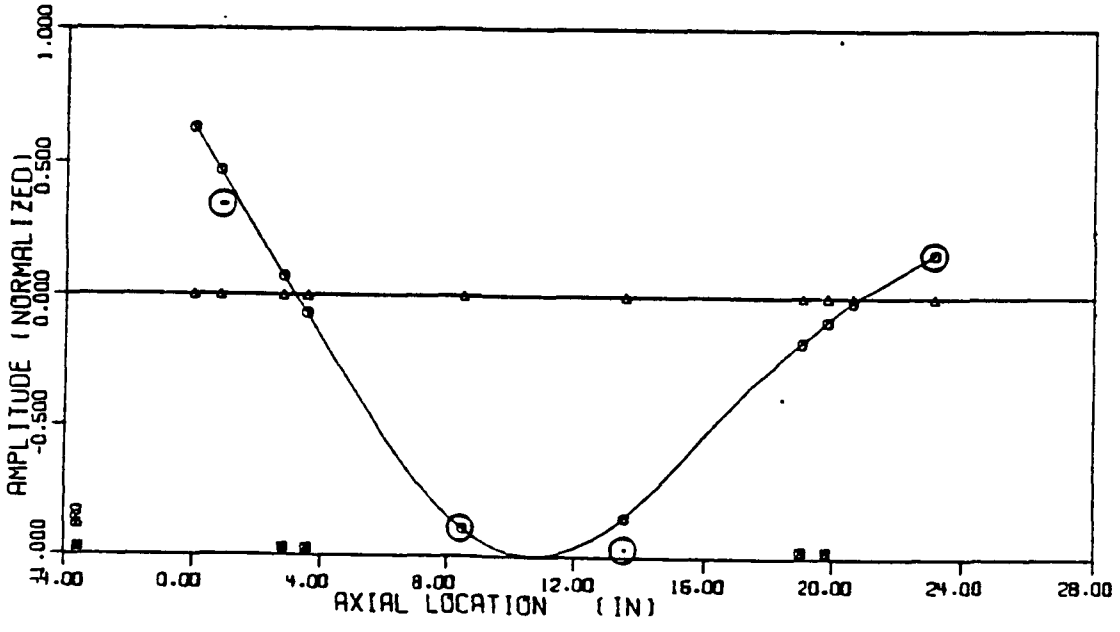

⊙ Measured at 21,500 rpm

85633

Figure 3-10 Mode Shape Comparison - Second Mode

Two support configurations which gave good potential low-speed balance "windows" were selected from the low-speed balancing assessment. One was to use the supports which simulated the HPOTP mode shapes. The second was to use supports which were more flexible on the disk end of the rig. The low-speed flexible balance assessment for these two configuration regions are shown in Figure 3-11. The results presented in this figure were used to determine the actual balance test points. For example, with the HPOTP mode shape simulator supports, the low-speed flexible balancing window is predicted to begin at approximately 8,000 rpm.

In summary, the test rig was modelled as a three-level system, and the model was used to determine critical speeds and low-speed flexible balancing "windows". A discussion of the test method and test results is given in the next section.

3.3 Test Results

The test rig described in the previous sections was assembled and used to evaluate the effectiveness of the low-speed flexible rotor balancing method. Initially, the rig was assembled in the test lab and instrumentation was calibrated and installed. During testing, laboratory equipment was used to continually monitor rig performance. This equipment included oscilloscopes for the displacement probes, an FFT analyzer with a channel selector switch, and thermocouples with temperature readouts to monitor lubricating oil. The FFT was also used in conjunction with a digital plotter to generate amplitude vs. speed plots. A computer data acquisition system was used for acquiring balance data. This MTI laboratory system consists of a PDP 11/03 mini-computer coupled with an analog-to-digital converter board. Several MTI programs available on the PDP 11/03 were used for acquiring vibration data (i.e., synchronous amplitude and phase) from the displacement probes. These data were used with a least squares influence coefficient balancing routine which automatically calculates correction weights.

For initial debugging, the test rig was run with hard mounts (i.e., the spring cartridges were not used during this phase). This configuration was used to debug the lubrication, instrumentation, and data acquisition systems. No major difficulties were encountered during these runs except that the maximum speed of

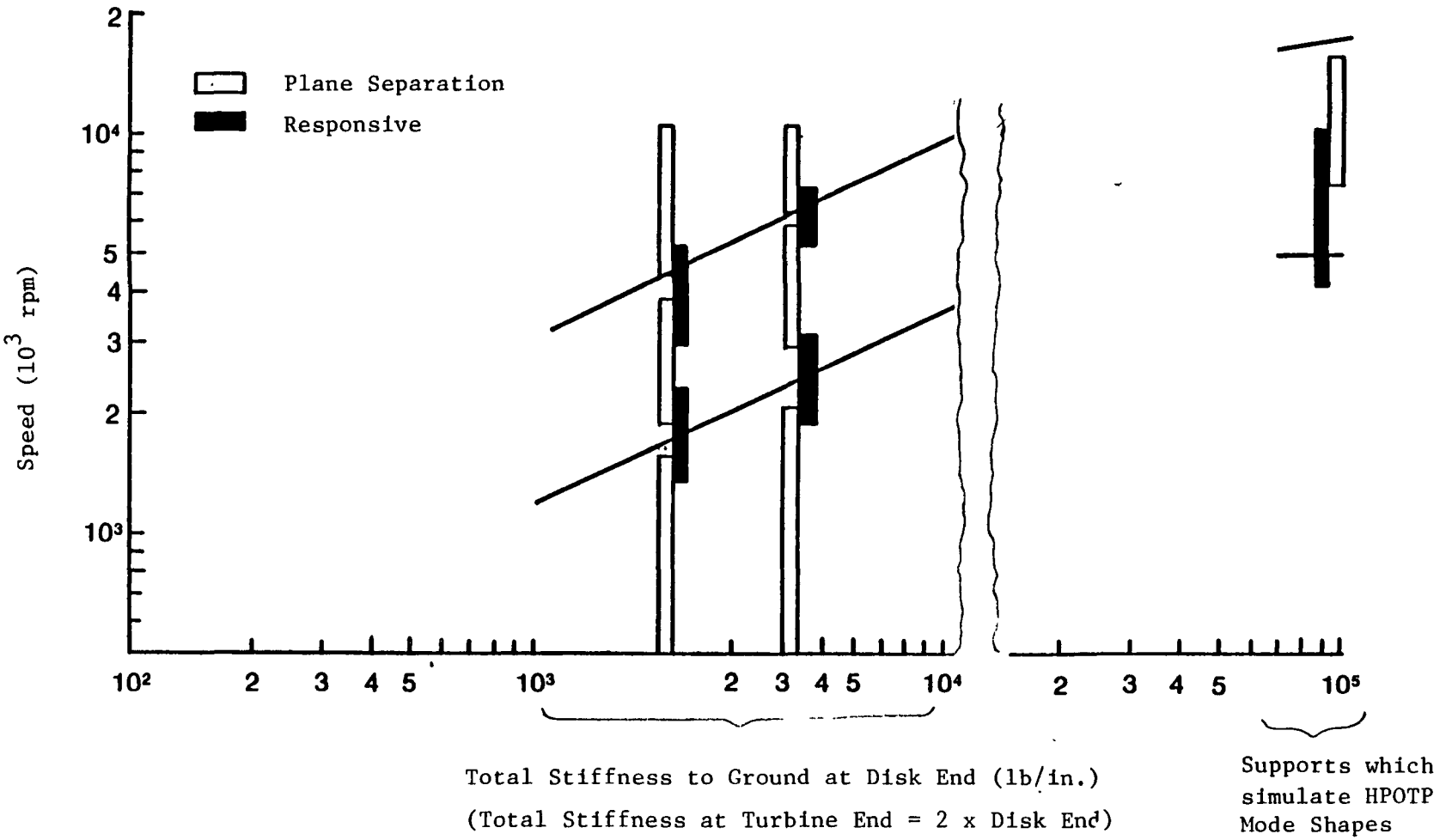

Figure 3-11 Test Rig Low Speed-Flexible Balancing Map

85612

24,000 rpm could not be reached. However, with the hard mounts there was misalignment between the bearings which increased power losses and limited maximum rig speed. When this initial debugging was completed and the spring cartridges were installed, maximum speed could be attained.

With the initial debugging completed, the first spring cartridges installed were those for which the test rig mode shapes are similar to the HPOTP (See Figures 3-9 and 3-10). During one of the initial runs on spring mounts, a change in response and critical speed was observed for no apparent reason. Immediately after this change occurred, an inspection of the rig revealed that one of the spring washers had failed. This washer was apparently overstressed due to excessive amplitude at the bearing pedestal. In all runs following this, motion at the bearing pedestal was carefully monitored and a lower level of response was maintained. As a result, there were no subsequent spring washer failures.

The debugged rig was then used to assess the effectiveness of the low-speed flexible balancing method by performing balance runs for several different spring supports. In each case, the same basic test procedure was followed. The test steps were:

1. Acquire low-speed runout data

2. Acquire uncorrected rotor data (i.e., no correction weights in the rotor) at various speeds

3. Install trial weights in the selected balance planes at the speeds from Step 2

4. Acquire trial weight response data

5. Calculate influence coefficients

6. Use the influence coefficients and baseline data to predict correction weights

7. Install the predicted correction weights and measure residual response

Several rig support configurations were used to assess different aspects of the low-speed flexible balancing method. As summarized in Table 3-3, a total of three different configurations were tested (referred to as I, II and III). The remainder of this section discusses these configurations and includes discussions of the test objective, test data and summary of results.

Test Configuration I consisted of support stiffness which simulated the HPOTP mode shapes. Based on the low-speed flexible balancing analysis of the rig in these supports, the predicted minimum low-speed flexible balancing speed was 8,000 rpm. The objective of these tests was to balance at different speeds below and up to 8,000 rpm, and compare the results to uncorrected rotor data. The balance speeds were:

- 2,500 rpm
- 5,000 rpm
- 7,500 rpm
- 8,000 rpm (predicted optimum)

A second test objective with the rig in this configuration was to perform high-speed influence coefficient balancing for the first and second critical speeds. The questions to be addressed with these test results were:

1. Will the method work at the predicted optimum speed?

2. Can successful balancing be performed at lower speeds on these supports?

3. How does low-speed flexible balancing compare to high-speed influence coefficient balancing?

A summary of the test rig Configuration I is shown in Figure 3-12 and the test results are shown in Figures 3-13 through 3-17. Figure 3-13 shows the results for low-speed balancing performed at 2,500 rpm. Balancing at this speed was unacceptable for operation at all speeds. In particular, response at the first critical speed after balancing was greater than response before balancing. For this particular run, there was significant 2/rev response while running above the first critical. This may have been caused in part by the large amplitudes,

TABLE 3-3

SUMMARY OF TEST CONFIGURATIONS

Configuration	Figure	Purpose
I	3-12	Low speed flexible balance with simulated HPOTP mode shapes
II	3-18	Assess effectiveness of low-speed flexible balance weights when HPOTP first critical speed location is simulated
III	3-20	Reduce low-speed flexible balancing speed

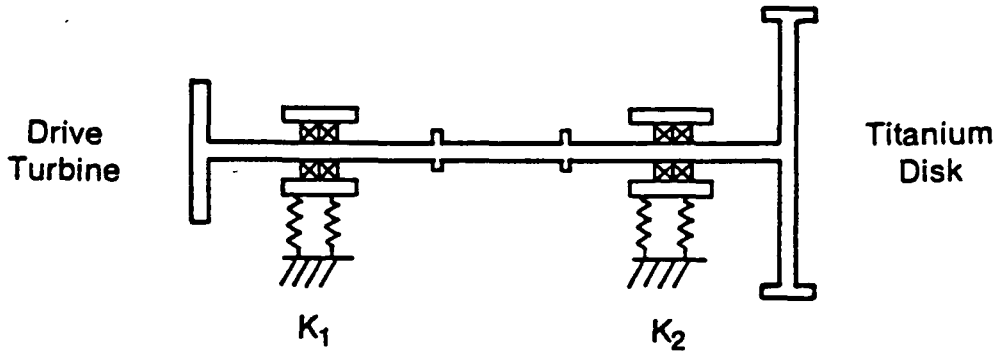

Total Radial Support Stiffness (nominal design values):

K_1 = 100,000 lbs/in

K_2 = 20,000 lbs/in

Critical Speeds (RPM):			
	Predicted	Measured	Type
First	4,967	4,700	Flexible Disk Bounce
Second	23,550	23,400	Bending-Turbine Precession

Figure 3-12 Test Rig Configuration I

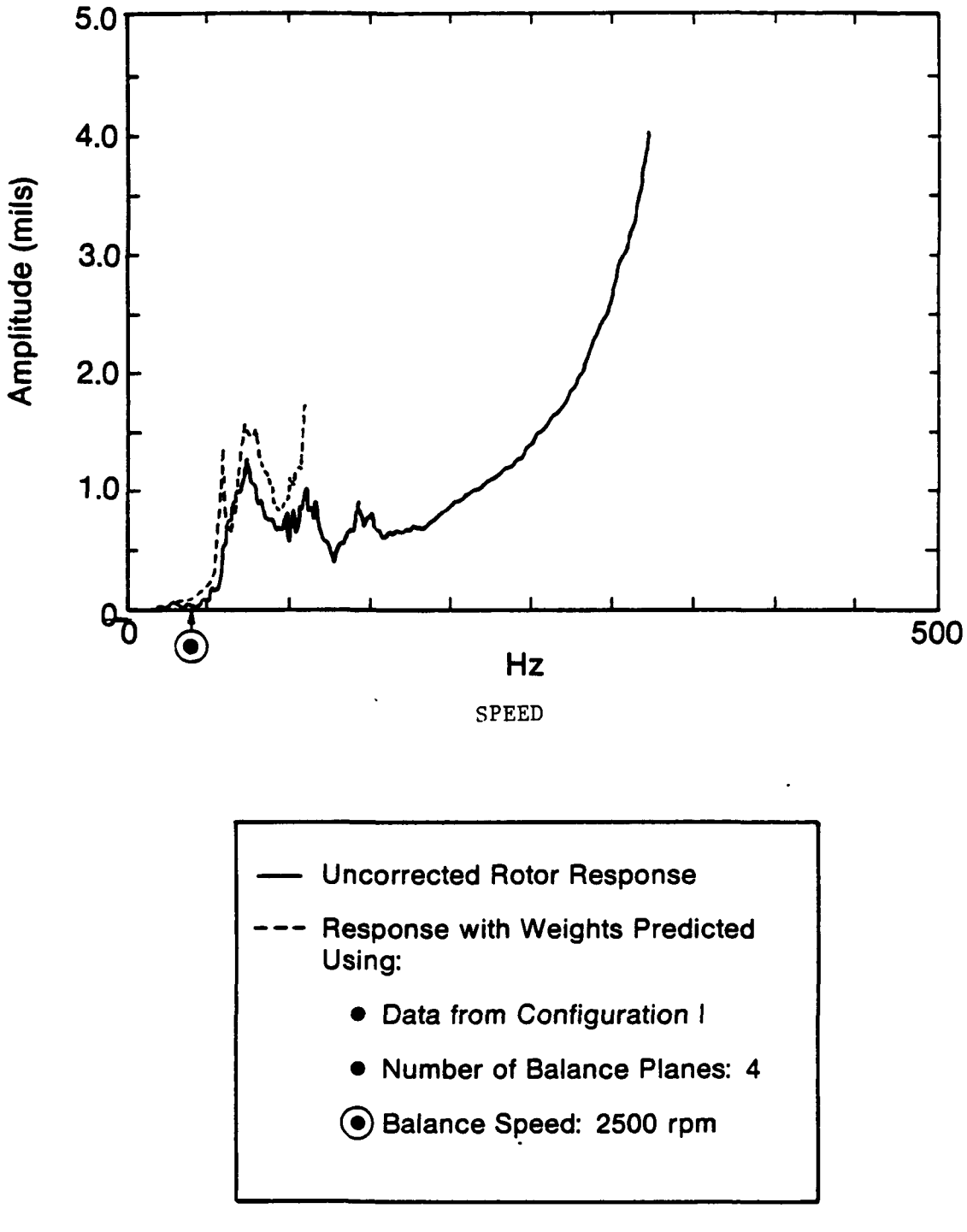

Figure 3-13 Rig Configuration I Center Probe Response Balance at 2,500 RPM

85595

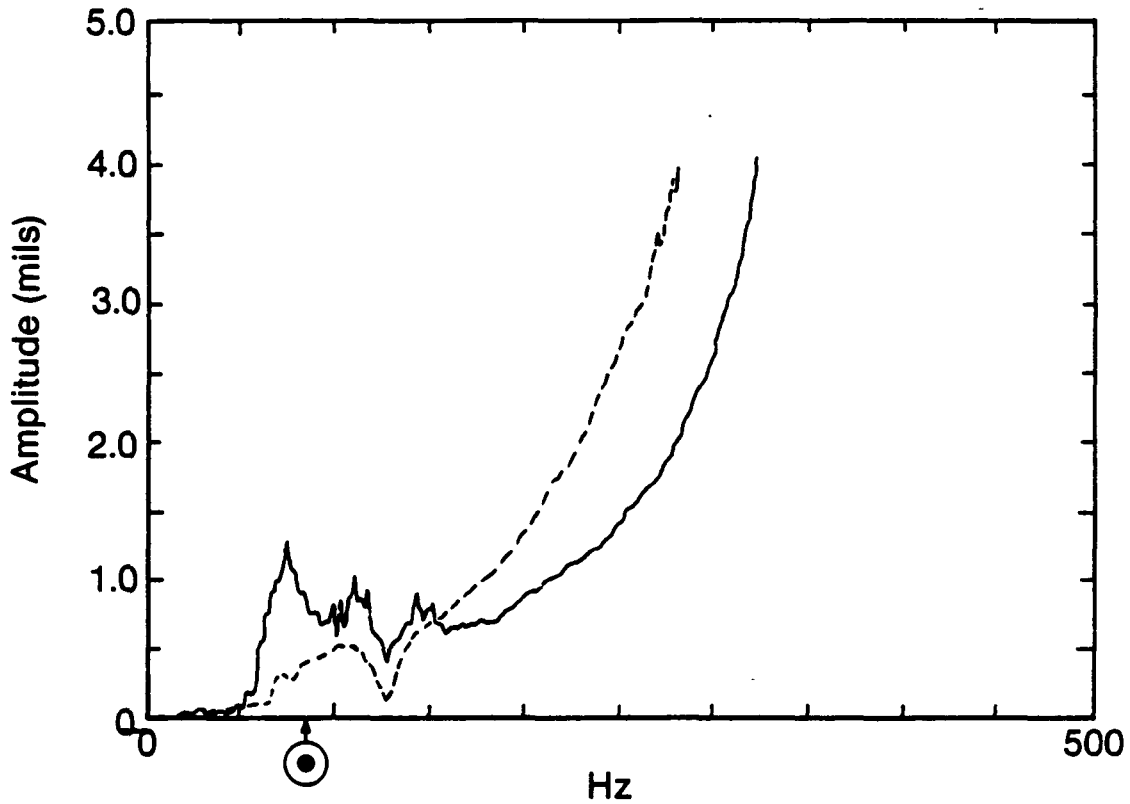

Figure 3-14 Test Rig Configuration I Center Probe Response Balance at 5,000 RPM

85597

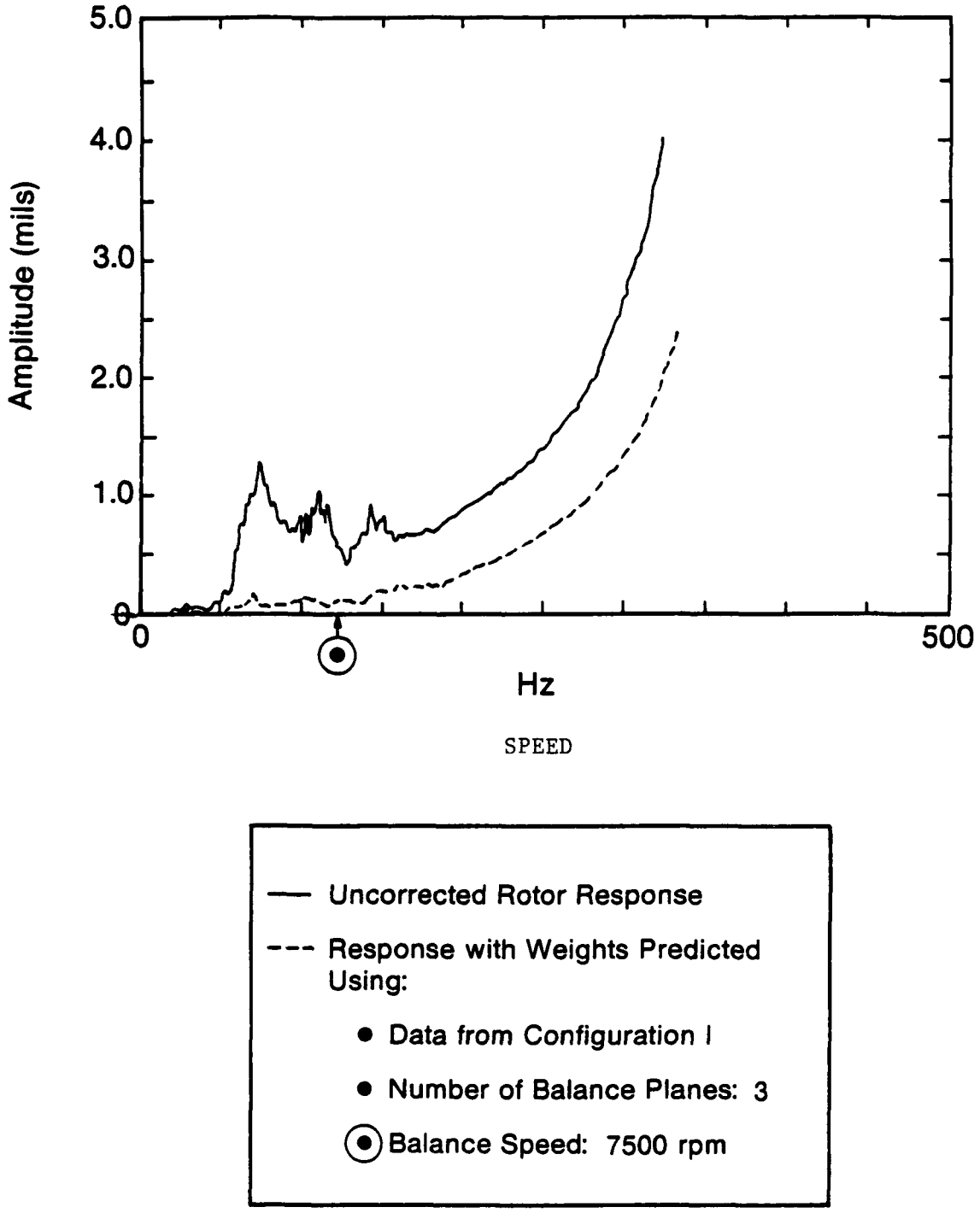

Figure 3-15 Test Rig Configuration I Center Probe Response Balance at 7,500 RPM

85598

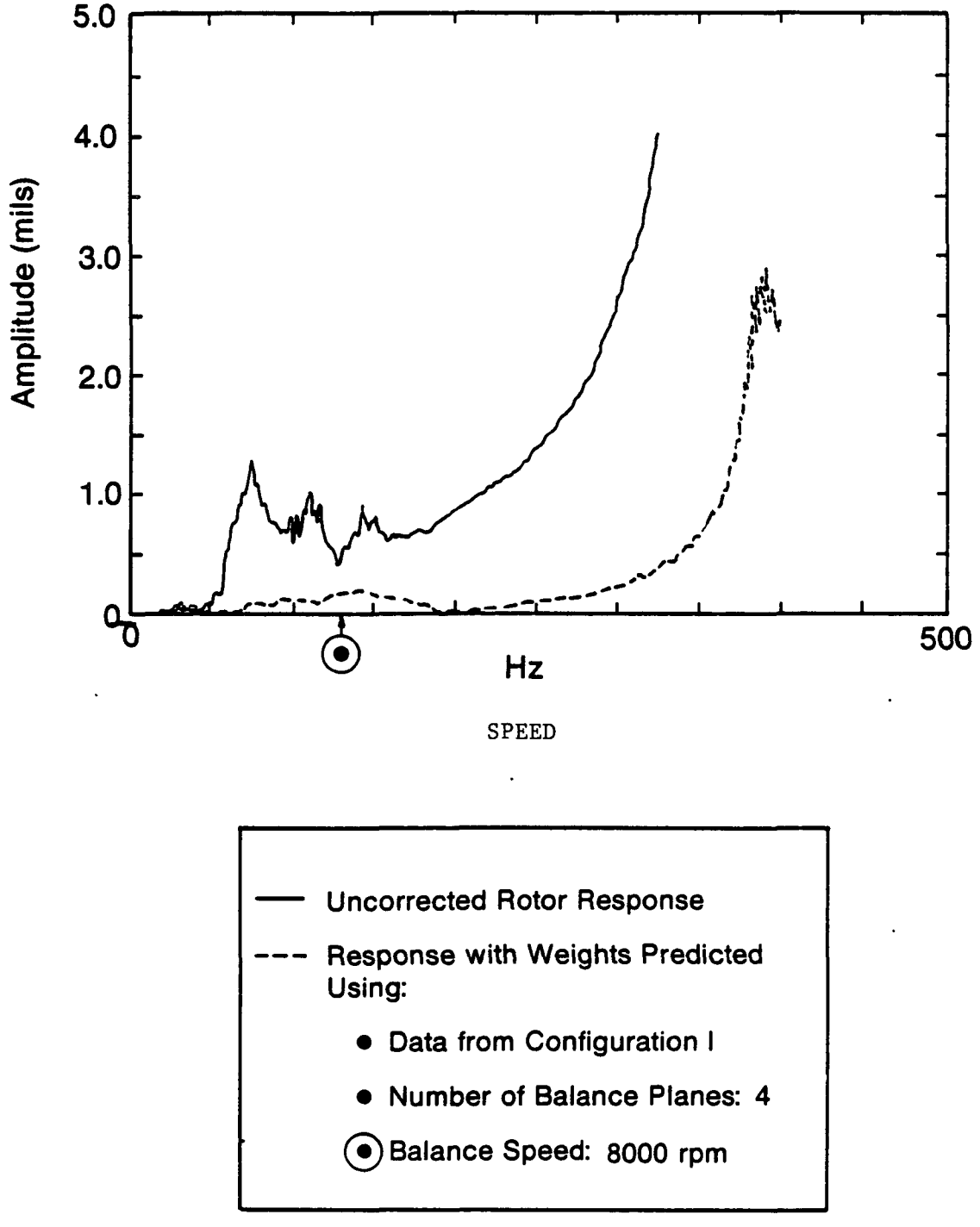

Figure 3-16 Rig Configuration I Center Probe Response Balance at 8,000 RPM

85596

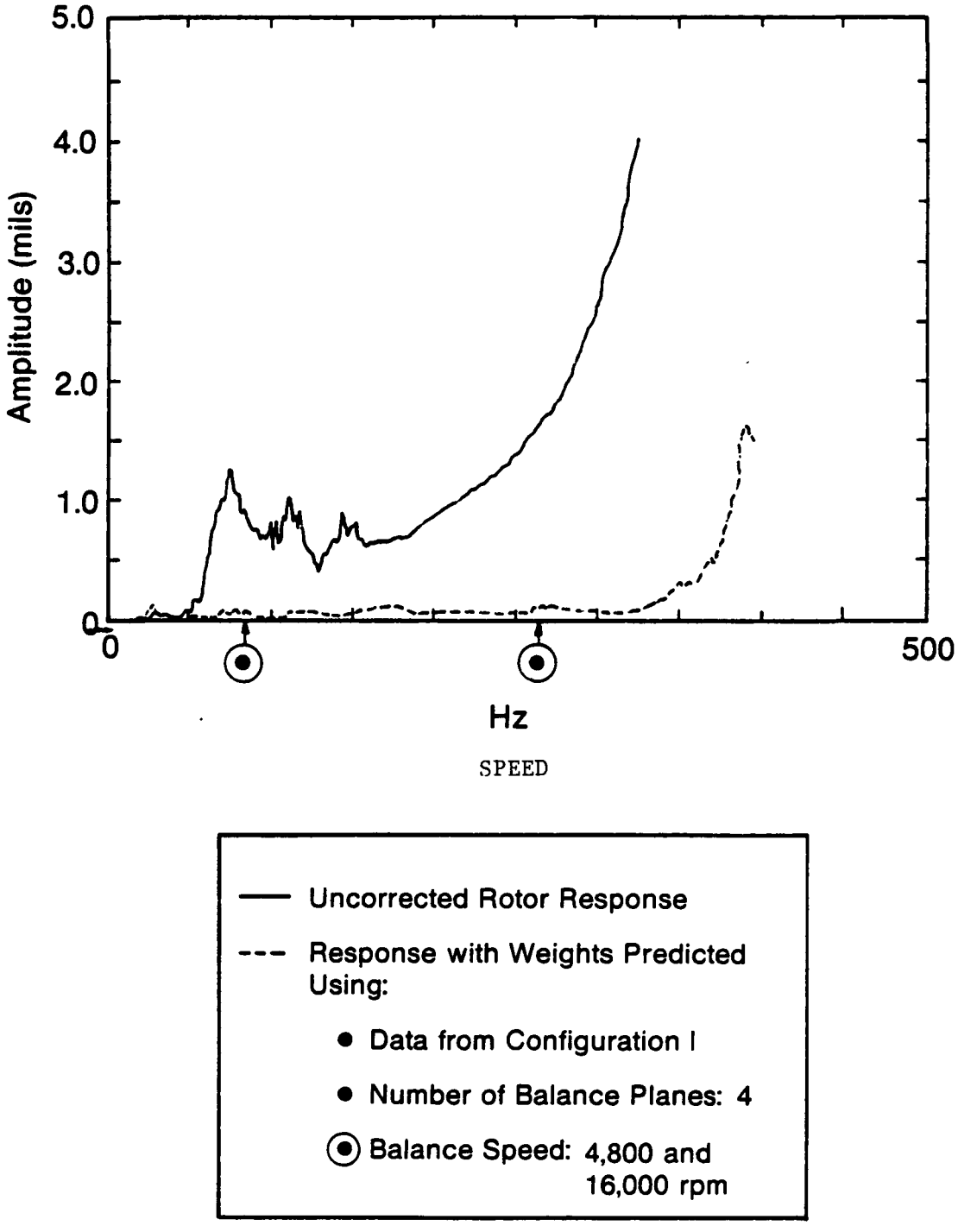

Figure 3-17 Test Rig Configuration I Center Probe Response High Speed Balance (4,800 RPM and 16,000 RPM)

85594

since the stiffness of the belleville washers can be nonlinear for large deflections. For all other runs, when response was smaller at the bearings, the response was primarily synchronous.

Figures 3-14, 3-15 and 3-16 show the "before" and "after" response for balancing at 5,000 rpm, 7,500 rpm and 8,000 rpm, respectively. These data show that as the balance speed is increased, the quality of balance (i.e., reduction in response) is also increased. In particular, for the balance at 8,000 rpm, it was possible to operate the rig above both the first and second critical speeds. For the balance at 5,000 rpm and 7,500 rpm, operation above the first critical was possible whereas operation above the second was not.

Finally, Figure 3-17 shows the balance results for two-speed influence coefficient balancing (i.e., high-speed balancing). For the two-speed balance it was possible to operate above both the first and second critical speed. Furthermore, the quality of balance is approximately the same as it was for the low-speed flexible balance at 8,000 rpm.

Following is a summary of results from the Configuration I tests:

1. Low-speed flexible rotor balancing at the predicted optimum speed results in satisfactory high-speed operation above the first and second critical speed

2. Balancing at speeds lower than the predicted optimum is not as successful

3. The quality of balance for low-speed flexible balancing is nearly the same as for high-speed influence coefficient balancing

For test rig Configuration II, which is shown in Figure 3-18, support stiffnesses of 100,000 lbs./in. were installed at each pedestal. The objective of using these supports was to simulate the location (i.e., speed) of the HPOTP first critical. In this configuration, the weights from Configuration I were installed and the following question was addressed:

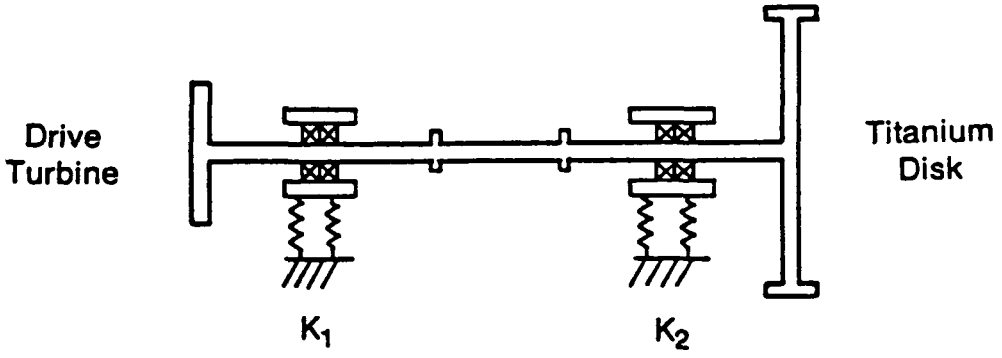

Total Radial Support Stiffness (nominal design values):

K_1 = 100,000 lbs/in

K_2 = 100,000 lbs/in

Critical Speeds (RPM):			
	Predicted	Measured	Type
First	11,358	12,100	Bending-Disk Precession
Second	25,104	>24,000	

Figure 3-18 Test Rig Configuration II

1. Are balance weights effective when the critical speed location is changed?

In terms of the HPOTP, this configuration assesses the effectiveness of using out-of-housing low-speed flexible balancing to minimize in-housing high-speed response. The balance results for Configuration II are shown in Figure 3-19. As this figure shows, before installing the correction weights, the maximum speed was limited to approximately 9,000 rpm. After installing the Configuration I weights (predicted at 8,000 rpm), it was possible to traverse the first mode and operate up to the maximum rig speed of 24,000 rpm. These data show that, for this system, the correction weights predicted using low-speed flexible rotor balancing supports are satisfactory for other supports. In terms of the HPOTP, this shows that out-of-housing low-speed flexible rotor balancing may significantly reduce in-housing high-speed response.

Configurations I and II demonstrated the viability of low-speed flexible rotor balancing and the potential applicablity to the HPOTP. Configuration III was planned and tested to address the following question:

1. Can the low-speed flexible balancing regime be reduced (i.e., can a successful balance be performed below 8,000 rpm?)

To address this question, Configuration III, as shown in Figure 3-20, was tested. In this configuration, the soft supports were installed in the titanium disk end pedestal. With these supports, balancing was performed at several different speeds. The results of these balance runs for 3,000 rpm, 5,000 rpm and 6,000 rpm are shown in Figures 3-21, 3-22 and 3-23, respectively. These data show that as the balance speed is increased the quality in balance (i.e., reduction in response) increases and this behavior is consistent with that seen in earlier Configuration I tests. In particular, for the balance at 3,000 rpm, it was not possible to operate above the first critical, whereas for the balance at 5,000 rpm and 6,000 rpm, it was possible to operate the rig above the first critical. Furthermore, with balance weights predicted at 6,000 rpm the maximum attainable speed was 21,000 rpm. These results show that it is possible to reduce the low-speed balance regime by changing the support flexibilities.

Finally, Configuration I was retested to address the following questions:

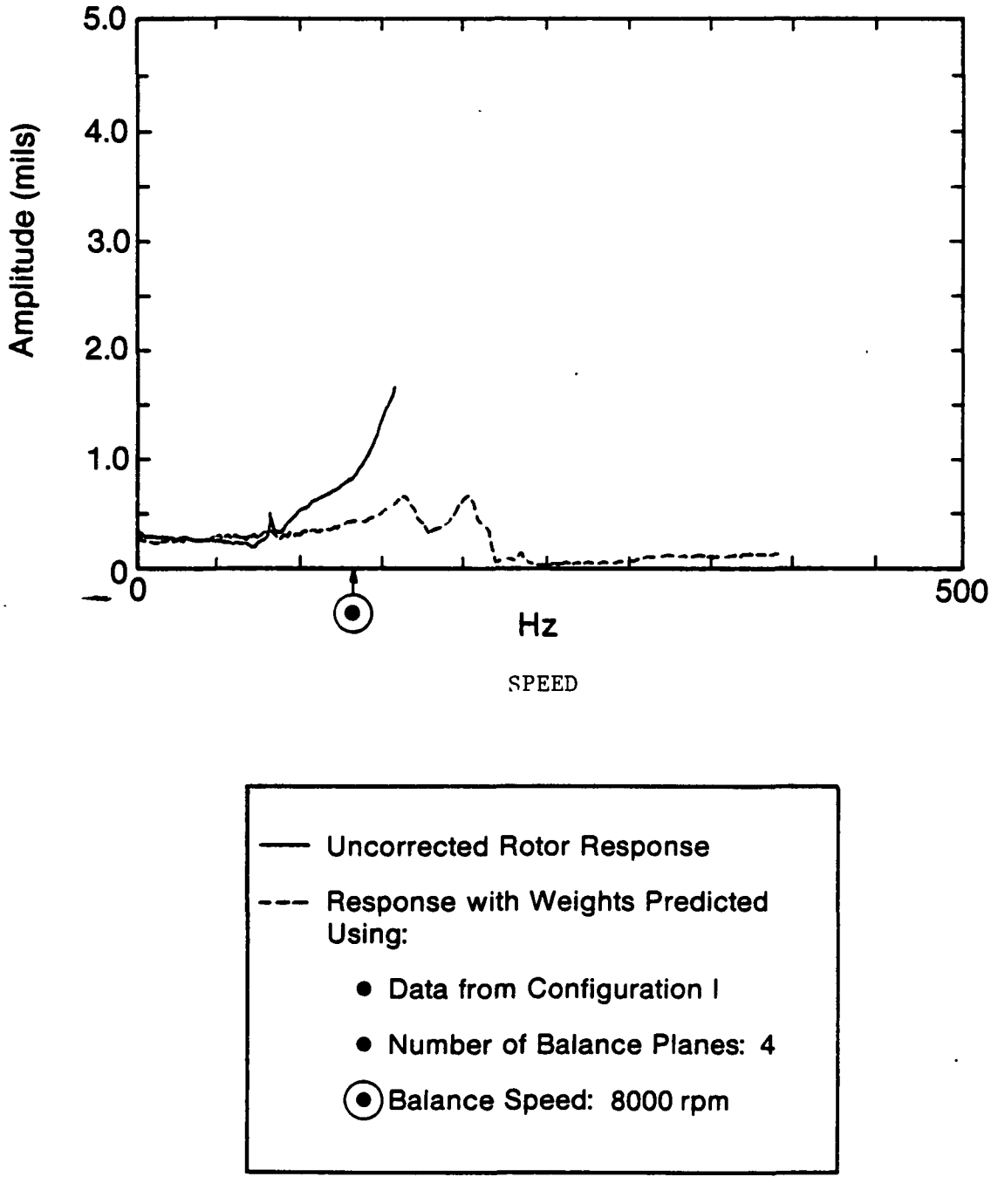

Figure 3-19 Test Rig Configuration II Titanium Disk Probe Response Balance at 8,000 RPM

85604

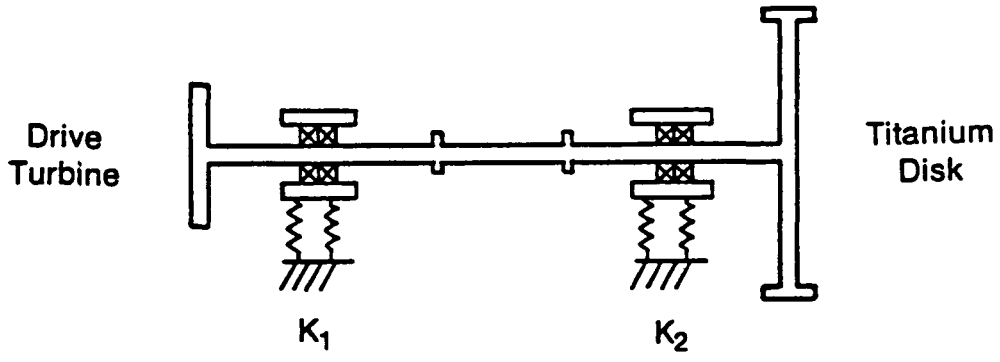

Total Radial Support Stiffness (nominal design values):

K_1 = 100,000 lbs/in

K_2 = 2,000 lbs/in

Critical Speeds (RPM):			
	Predicted	Measured	Type
First	1,830	3,300	Disk Bounce
Second	23,315	>23,000	

Figure 3-20 Test Rig Configuration III

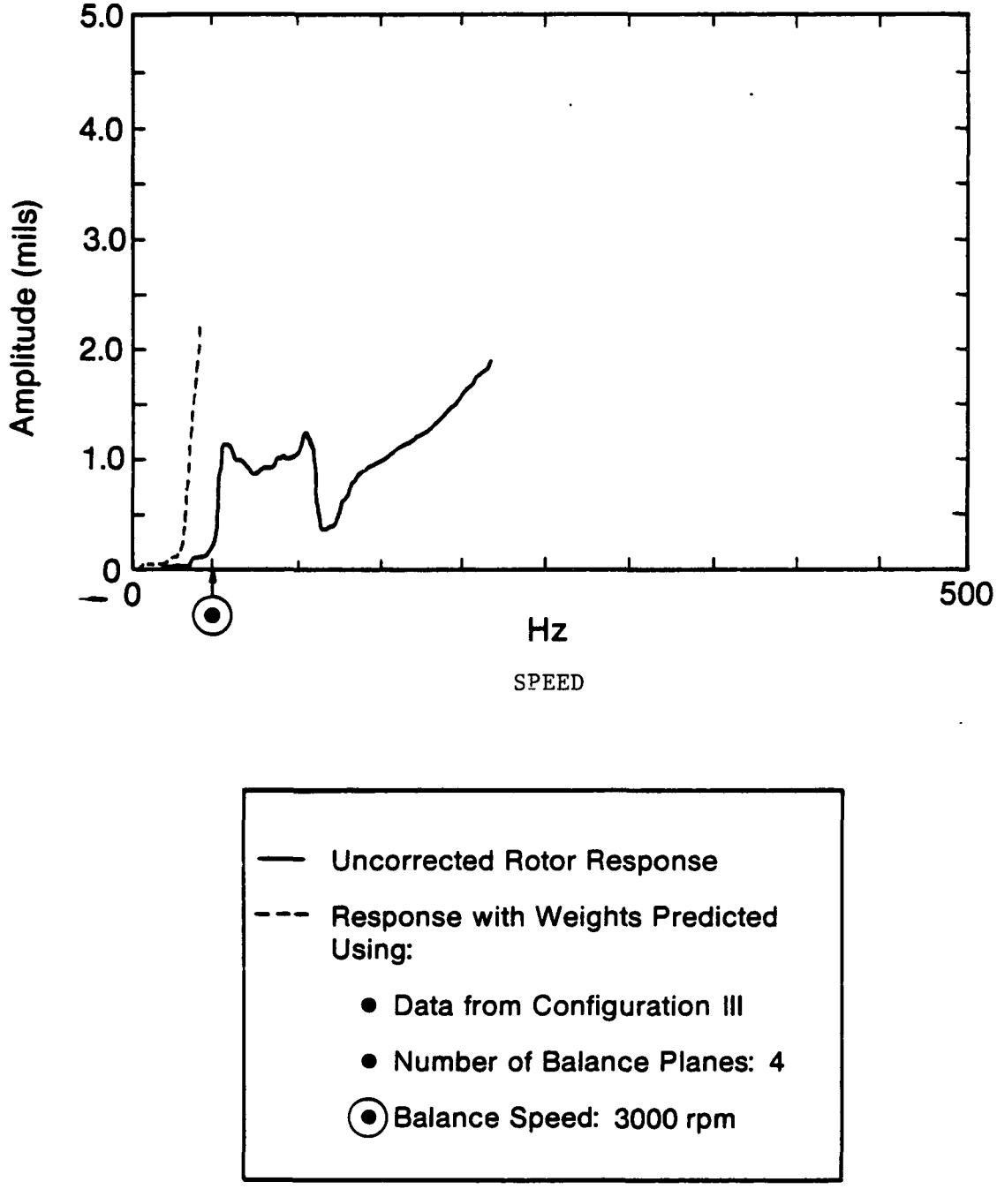

Figure 3-21 Test Rig Configuration III Center Probe Response Balance at 3,000 RPM

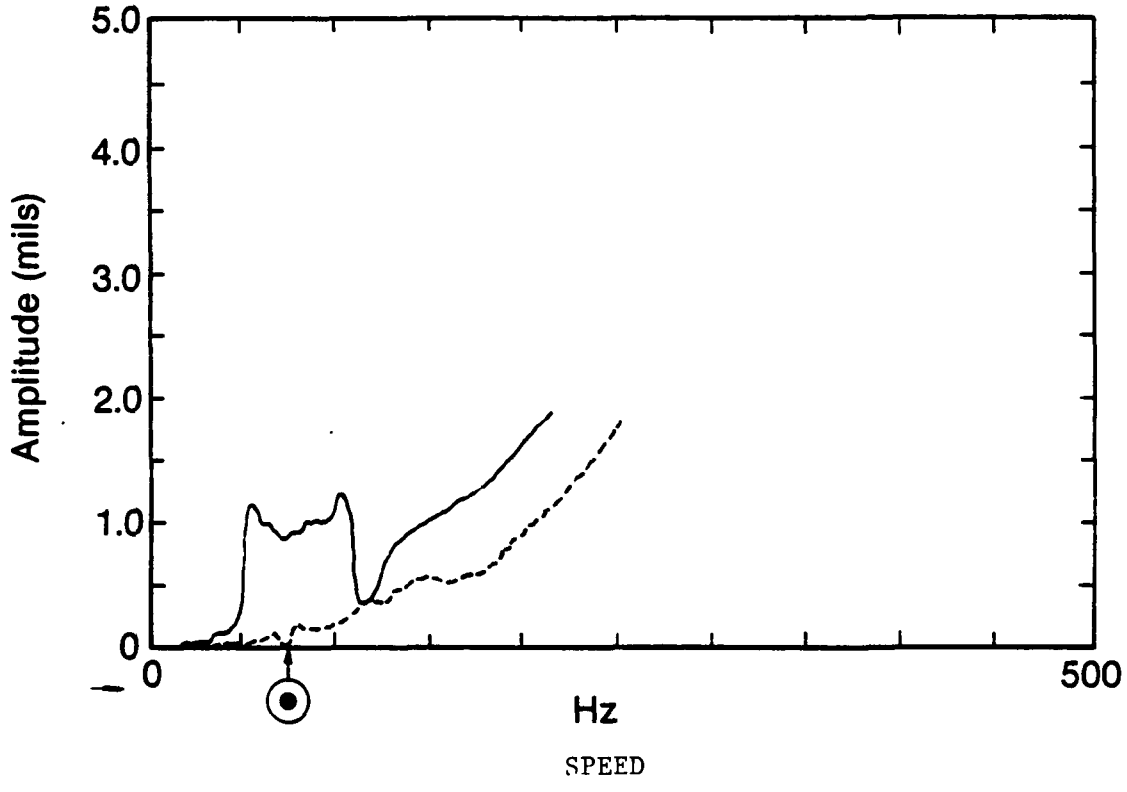

Figure 3-22 Test Rig Configuration III Center Probe Response Balance at 5,000 RPM

85605

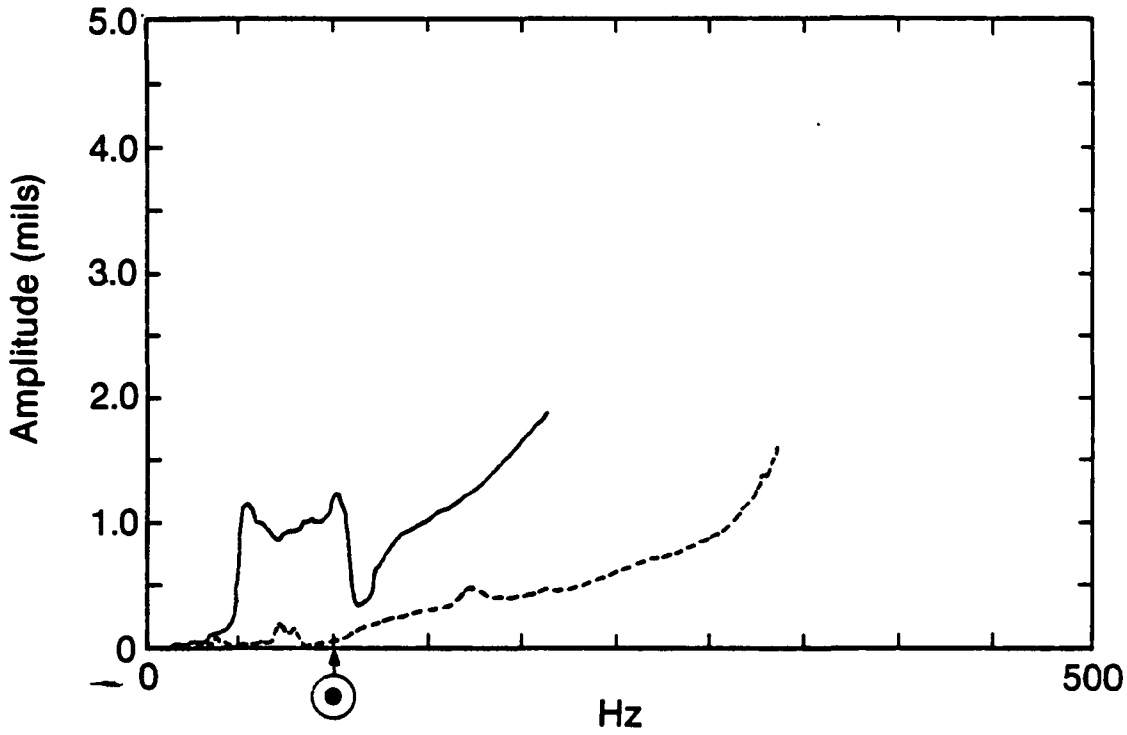

Figure 3-23 Test Rig Configuration III Center Probe Response Balance at 6,000 RPM

85600

1. Do balance weights predicted with low stiffness also balance Configuration I?

2. Do rigid body balance weights balance Configuration I?

The results from the Configuration I retest are shown in Figures 3-24 and 3-25. In this retest, the weights predicted at 6,000 rpm from Configuration III were installed. As shown in Figure 3-24, with these weights it was possible to traverse the first critical speed and a maximum speed of approximately 22,000 rpm was reached (essentially the same speed as with the Configuration III supports). This shows that these weights are effective but that the quality of balance was not as good as with those predicted at 8,000 rpm weights.

Finally, a two-plane low-speed rigid body balance was performed and the weights were installed in the rotor. Figure 3-25 shows that the rigid body balance weights produced little change in the first mode maximum amplitude and that the maximum speed was limited to 20,000 rpm. Thus, for this hardware, rigid body balancing is not effective for high-speed operation.

In summary, a series of tests have been conducted to evaluate the low-speed flexible rotor balancing method, and compare the results with those from high-speed flexible rotor and low-speed rigid body techniques.

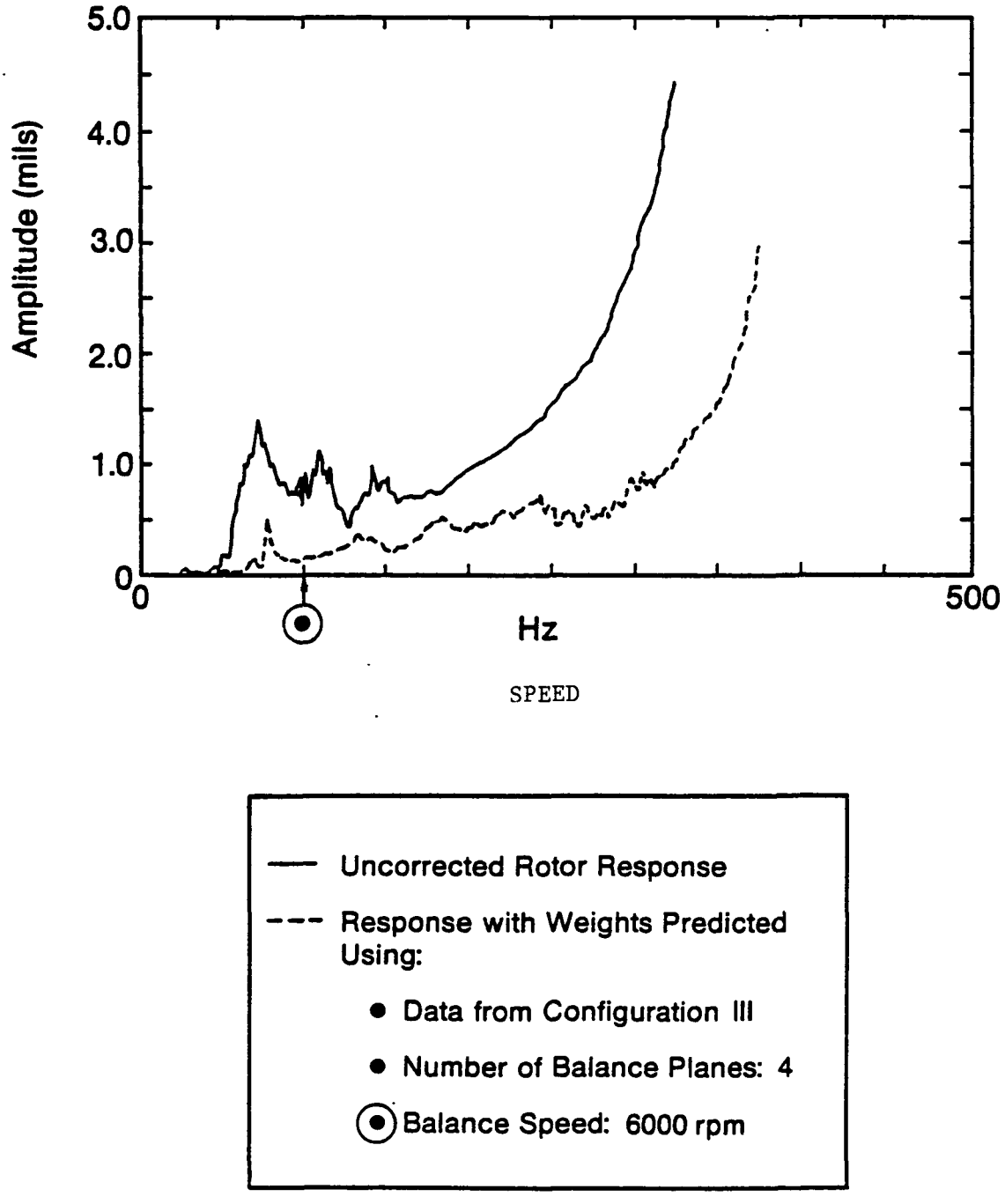

Figure 3-24 Test Rig Configuration I Center Probe Response Balance at 6,000 RPM

85599

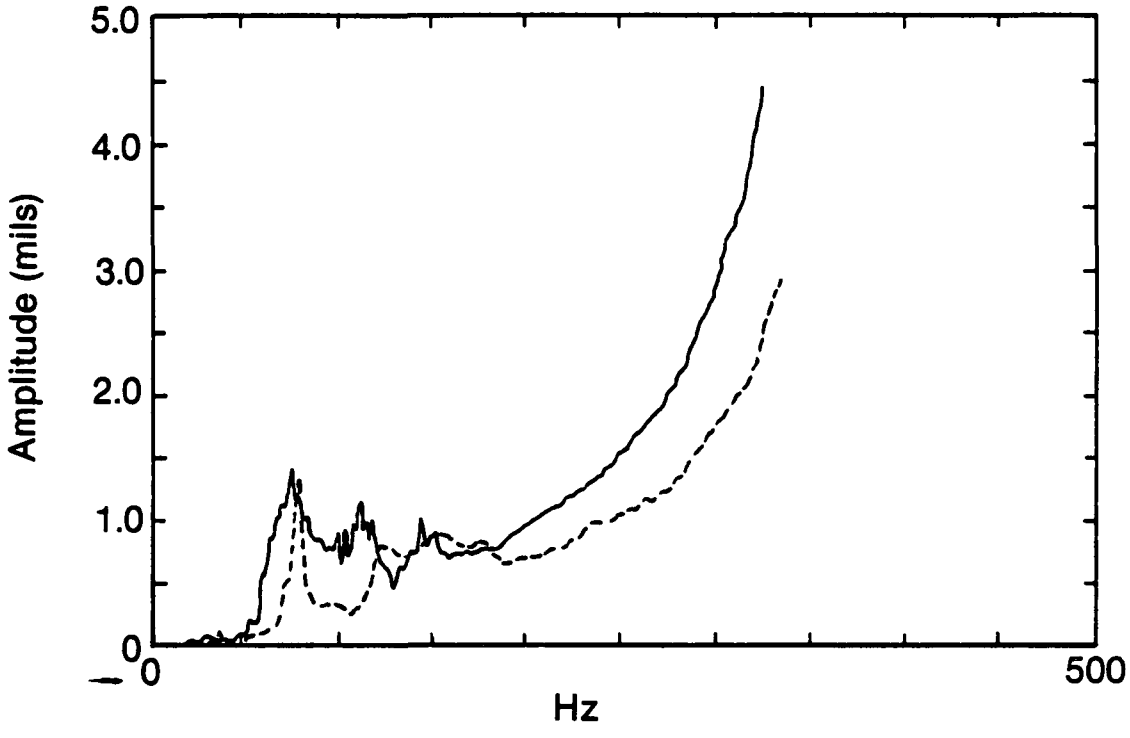

Figure 3-25 Test Rig Configuration I Center Probe Response Rigid Balance

85603

4.0 CONCLUSIONS AND RECOMMENDATIONS

4.1 Conclusions

A method for determining low-speed flexible balancing "windows" has been established and demonstrated in the laboratory using a flexible rotor rig. These "windows" are combinations of support stiffness, balancing speed and probe and balance plane locations which, when combined with probes of sufficient sensitivity and a suitable existing balance weight computation method, allow true flexible rotor balancing to be performed at low speeds. Major conclusions from the test data show that:

- Low-speed flexible rotor balancing is a viable technology.
- The quality of balance achieved with low-speed flexible rotor balancing is roughly equivalent to high-speed flexible balancing.
- For the test rig used, successful low-speed balancing required operation above the first mode.
- Lowering the location of the first mode reduces the speed at which satisfactory balancing can be achieved.
- Balance speed/stiffness regimes predicted using the low-speed flexible rotor balancing approach are generally consistent with analytic predictions.
- Rigid body balance was found unacceptable for satisfactory high-speed operation.
- Correction weights predicted using the flexible supports required for low-speed flexible rotor balancing are acceptable for different support stiffnesses.

These test results show that the low-speed flexible method is a viable technology for balancing at low speed to ensure smooth, high-speed operation. Furthermore, by judicious implementation of this methodology, the range of balance

speeds can be controlled and the state of balance achieved can be satisfactory for different flexibilities. Therefore, if applied to the HPOTP, the low-speed flexible rotor method may provide a means for low-speed, out-of-housing balancing, which results in smooth, high-speed operation.

4.2 Recommendations

Based on the success of the proof-of-principle tests, further implementation of this method for the HPOTP is recommended. Implementation should include refinement and qualification of the method for the HPOTP, and development of a finalized system for out-of-housing balancing of HPOTPs.

Prior to development of a finalized balancing system, the method should be qualified in a laboratory environment. Qualification testing should use actual HPOTP rotor hardware or hardware that simulates HPOTP rotordynamic performance. Furthermore, qualification tests should be planned to evaluate the effectiveness of the method for different balance speeds and suspension characteristics. In addition, these tests will identify specific hardware requirements (such as required support flexibility) and computer hardware/software requirements for a finalized HPOTP low-speed flexible rotor balancing system.

General requirements of a system for qualification testing and for the finalized HPOTP balancing system are similar. One difference is that the qualification system can use a test shaft which simulates the rotordynamic performance of the HPOTP whereas the finalized balancing system will use actual HPOTP rotor hardware. In addition, the rig for qualification tests must have high-speed capability for performing verification tests at maximum HPOTP speeds whereas the system for balancing production HPOTPs need only operate at the low-speed flexible balancing speeds. The remainder of this section contains system specifications and requirements for the following components:

- Mechanical Hardware
  - Drive system
  - Bearing Lubrication
  - Bearing Suspension

- Computer/Data Acquisition Hardware
  - Instrumentation
  - Mini/Micro Computer
  - Analog-to-Digital Converter
- Software Architecture
  - Control
  - Data Acquisition
  - Calculation
  - Output/Graphics

4.3 Mechanical Hardware

Drive systems for use during qualification testing and for the finalized system for balancing production HPOTP rotors are needed. The primary performance requirements of the drive systems for these two applications are somewhat different. For evaluation and high-speed verification tests using the HPOTP rotor simulator, the drive system must have a maximum speed of 35,000 r/min. On the other hand, the maximum speed for balancing production rotors is not as high, but quick acceleration and deceleration rates are required to limit bearing life expenditure.

A bearing lubrication method for the qualification test rig must be capable of lubricating and cooling (to avoid thermal distress to the 440C bearing material) the support bearings at the low-balance speeds as well as at the high verification speeds. In addition, the bearing lubrication method should be compatible with HPOTP bearing hardware. Note that the current bearing support design makes no provision for jet or mist-type lubrication, since the bearings are bathed in LOX. Hence, the envelope available for qualification rig support bearing cooling and lubrication is extremely limited. Little room exists for admitting oil to, and scavenging it from, the bearings and careful engineering of this system will be required. For the finalized balance system, the bearing lubrication method must lubricate and cool the bearings at the low-speed flexible balance speeds. Furthermore, it must be a method which uses only LOX-compatible materials, therefore, judicious selection of a lubricant is required.

A suspension system for the qualification test rig must have the range of flexibility needed to perform low-speed flexible balancing as well as to simulate the in-housing suspension of the HPOTP. Other design objectives include satisfactory fatigue life, repeatability, ease of assembly/disassembly, linearity and lack of a deadband.

One approach for meeting suspension system requirements consists of a cartridge between the bearing outer race and bearing pedestal. Within this cartridge are removable spring elements similar to those in Figure 3-2 and 3-3. Such an arrangement can be redesigned to allow for a wide range of spring stiffness, long fatigue life and good repeatability. Furthermore, such a suspension system can be easily incorporated into the final design of the low-speed flexible balancing system for production HPOTPs.

4.4 Computer/Data Acquisition Hardware

For successful low-speed flexible balancing the ability to measure low levels of rotor-bearing response is required. In particular, balance data will usually be required at relatively low speeds that are not at rotor-bearing criticals, so that little dynamic amplification occurs. One way to accurately measure these low response levels is with high sensitivity vibration sensors and a mini-computer-based data acquisition system. Key hardware components required for such a system are shown in Figure 4-1. It is recommended that hardware be selected which can be used for verification tests as well as for the finalized system.

Vibration sensors with high accuracy need to be used and their support structures integrated with the overall mechanical design. Both shaft displacement and bearing force measurement systems can be considered. There are several types of instrumentation systems available for measuring shaft displacement. *Eddy current proximity probes, fiber-optic probes, and capacitance probes are* often used for rotating equipment. The sensitivity of capacitance measurement probe and fiber optic measurement systems can be an order of magnitude greater than that of the eddy current. Thus, based on accuracy, the capacitance or fiber optic systems are better suited for low-speed flexible balancing than the eddy current probes. It is important to note that capacitance systems (such as MTI's Accumeasure System 1000 ™) can measure displacement with a resolution on

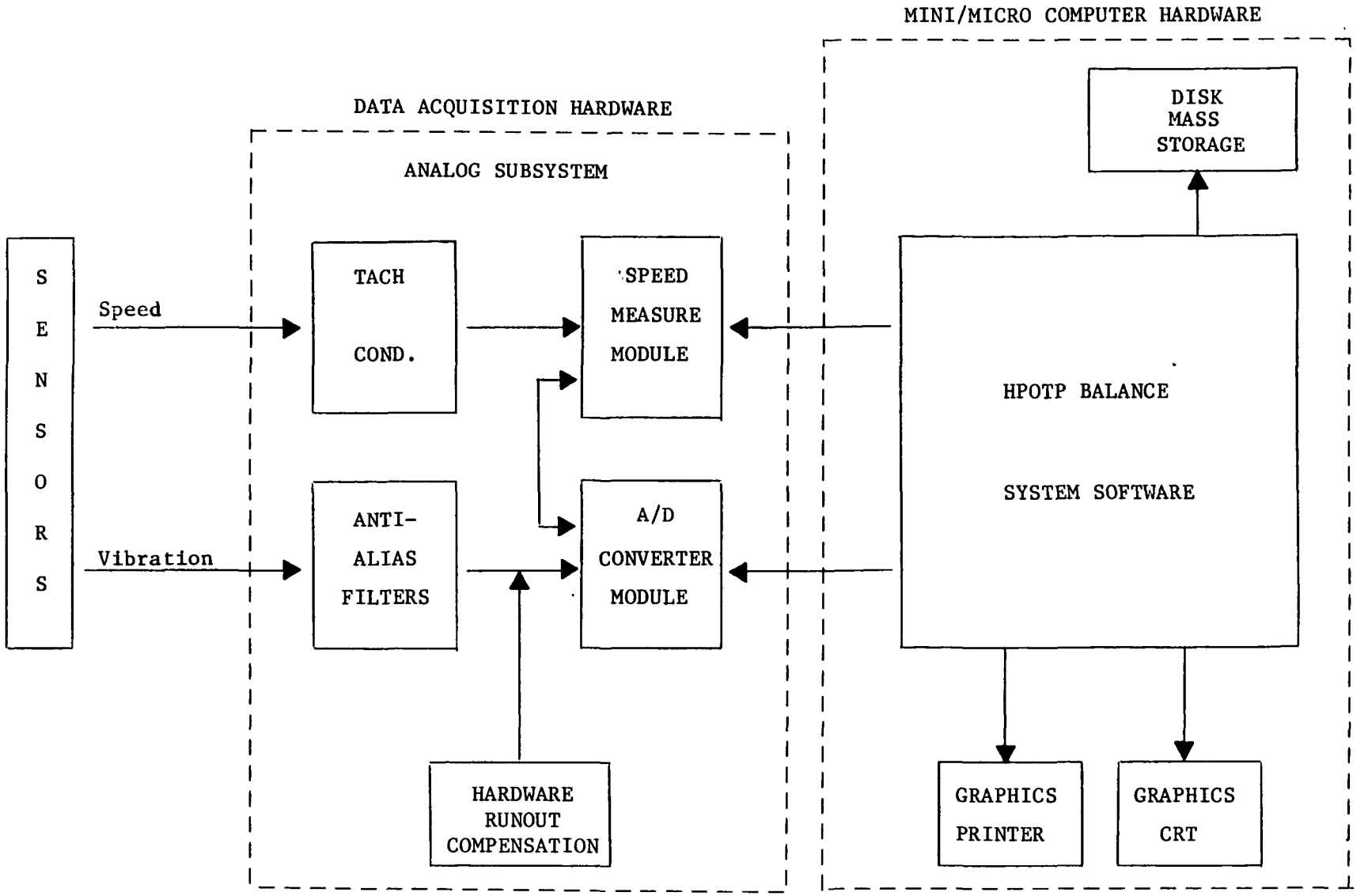

Fig. 4-1 NASA HPOTP BALANCE SYSTEM

the order of 0.05 mils. This is an improvement over the 0.5 mil resolution achieved with the instrumentation used on the test rig discussed in Section 3. For displacement measurement systems, mechanical and electrical runout can greatly exceed the small amplitude changes being sought, resulting in degraded measurement performance. Because this runout is generally repeatable, it can be measured and subtracted from the probe signals. This is best done using a "synchronous runout corrector", and such a device or its equivalent must be incorporated into the system.

In addition to shaft response measurement, it may be desirable to measure force transmitted through the bearings. If this is the case, a force transducer could be incorporated into the design of the bearing pedestals. A variety of transducers can be used for this application, including piezoelectric and/or strain gage types.

The vibration sensor signals generally need to be conditioned using low pass anti-alias filters. These filters are needed to limit the vibration signal bandwidth to ensure compliance with sampling requirements. The conditioned signals are then digitized using a high-speed, A/D converter circuit synchronized with the tachometer signal. The A/D converter will require at least 12-bit accuracy to read low levels of response.

Computer hardware requirements include a processor, terminal, printer and possible graphics plotter. During the selection of the computer system hardware components, consideration should be given to the following:

- Computational requirements (expected need: 16 bit cpu)
- Memory requirements (expected need: 256 Kb)
- Fixed mass storage requirements (expected need: 10-20 Mb Winchester)
- Removable storage
- Data acquisition requirements, trade-offs, and constraints
  - A/D speed
  - Resolution
  - Number of channels
  - Anti-alias filters
  - Frequency range of data
  - Allowed data collection times

- Data output requirements (printed, graphical, etc.)
- Computer hardware ruggedness and reliability
- Environmental factors (temperature, humidity, cleanliness, etc.).

4.5 Software Architecture

Modular software should be developed for verification testing and this software will form the basis for the finalized system software package. The required software components need to be designed, flowcharted, coded, debugged, integrated, and tested. The verification software should implement the major functions identified in Figure 4-2 and listed below:

- Balancing System Control
  - Menu-driven operator interfaces
  - Simple and easily understood command sequences
  - Production oriented balance sequence
  - Error message and self-recovery from error status
- Data Acquisition Control Software
  - A/D control
  - Speed measurement
  - Data sampling
  - Data collection sequencing
- Balancing Software
  - Influence coefficient calculation
  - Balance weight prediction
  - Balance weight constraints (i.e., weight removal limits)
  - Prescribed orbits
  - Use of previously determined influence coefficients
  - Determination of plane independence from empirical data
- Output Software
  - Balance reports
  - Plots

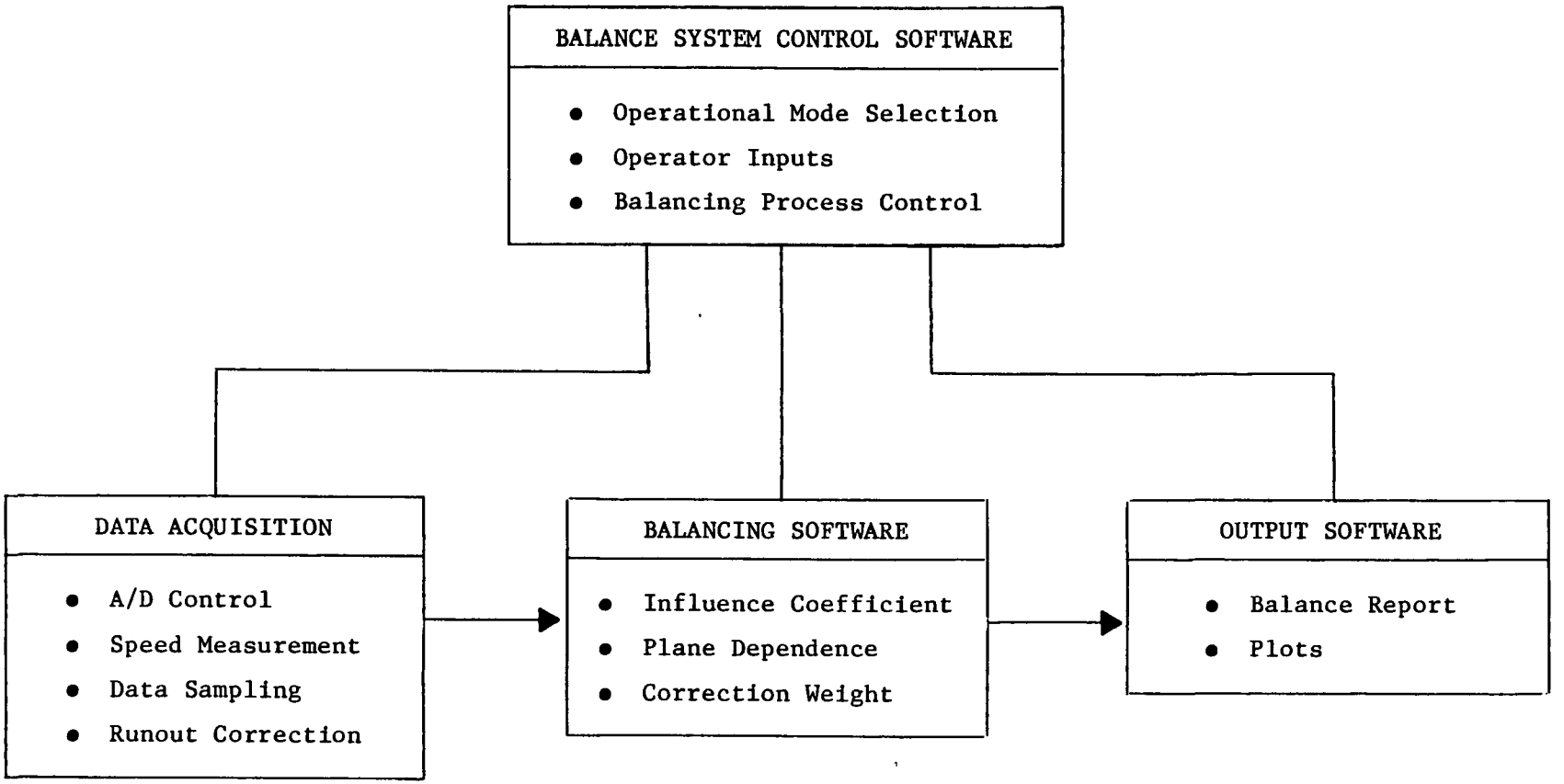

Fig. 4-2 Balance System Software Block Diagram

More details of each of these functions are shown in Figures 4-3 and 4-4.

The above recommendations outline a conservative approach to developing a finalized integrated system for low-speed flexible out-of-house balancing of HPOTP rotors. As described above, the four key elements of such a system are: 1) mechanical components, 2) instrumentation, 3) data acquisition hardware and 4) computer software. The challenge in developing an effective low-speed flexible balancing system for SSME turbopumps is the integration of these components and the judicious application of the low-speed flexible balancing analysis.

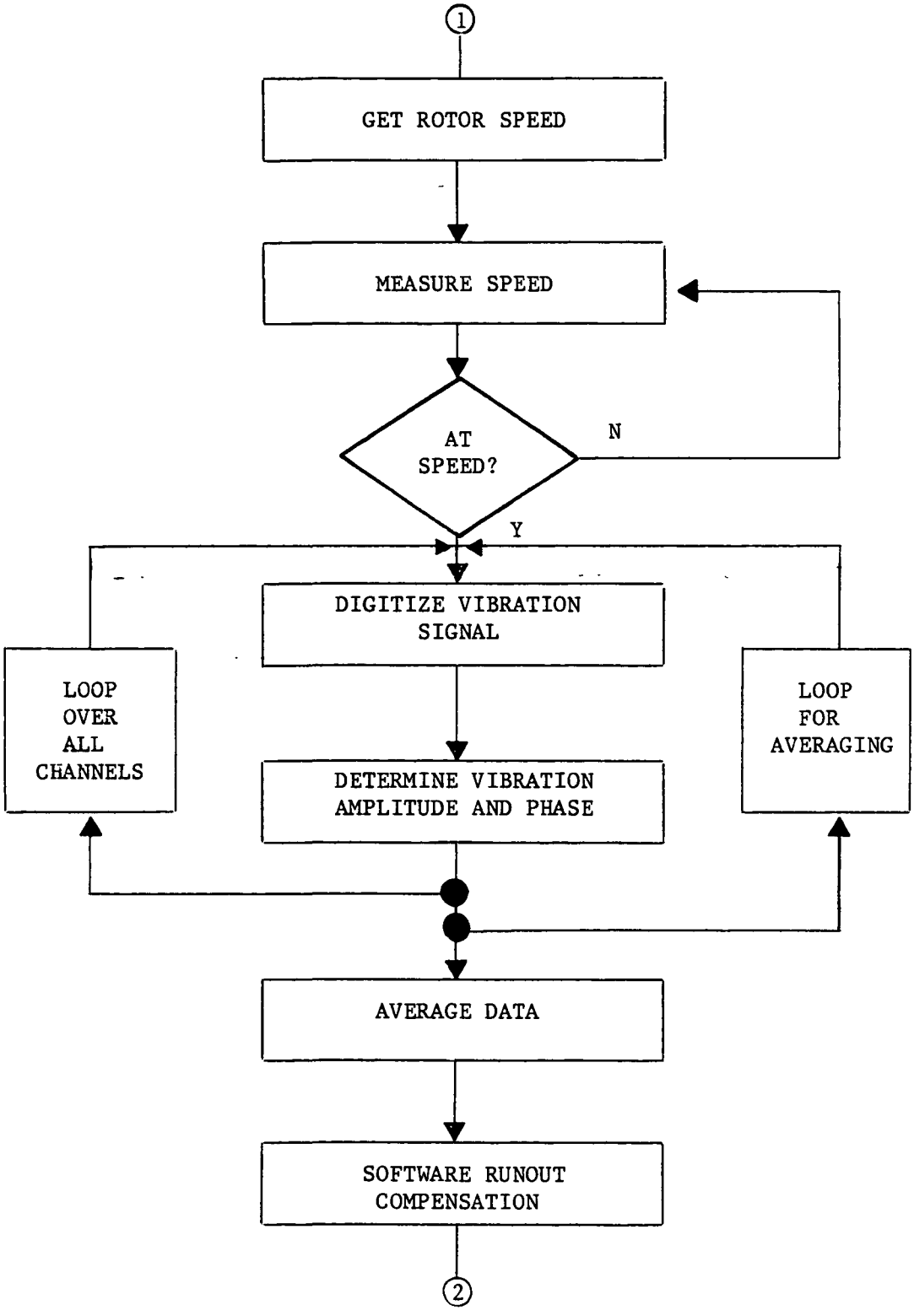

Fig. 4-3 Vibration Data Acquisition

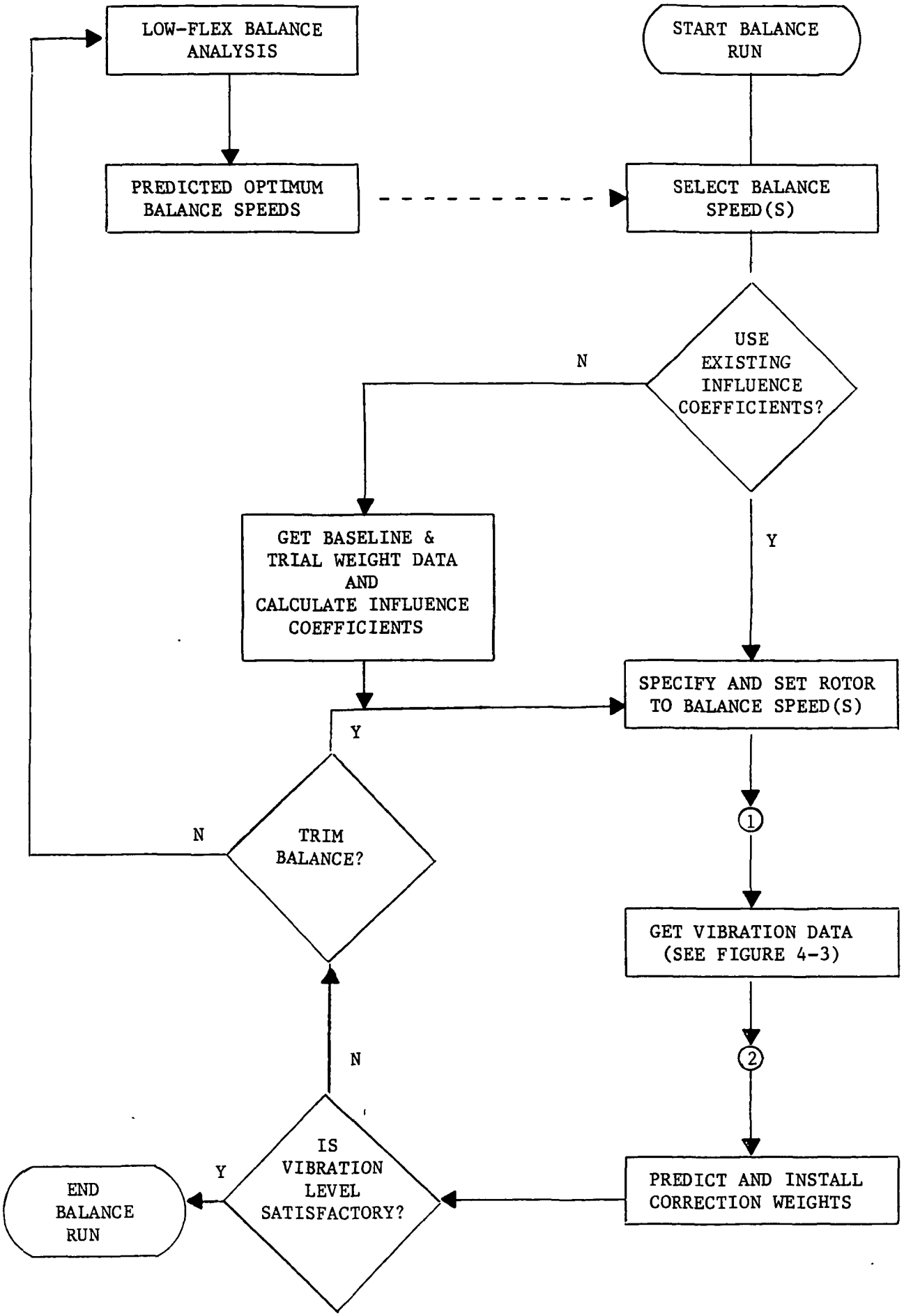

Fig. 4-4 Balance Sequence

5.0 REFERENCES

1. Darlow, M. and Zorzi, E., "Mechanical Design Handbook For Elastomers", NASA Contract Report 3423, June 1981.

APPENDIX A

Sample Computer Output for Test
Rig Critical Speed

Description	Pages
Summary of Input and Geometry	A-2 to A-14
Critical Speed Analysis Summary	A-15, A-16
First Critical Speed Mode Shape	A-17 to A-19
Second Critical Speed Mode Shape	A-20 to A-22
Third Critical Speed Mode Shape	A-23 to A-25

ECHO PRINT OF INPUT FILE

```
  TEST RIG MODEL
 LOT           1.
 ILE
 TABILITY
CRITICAL     0000.      50000.
POST
 ESPONSE
 NFLUENCE
 ALANCING
END1
MATERIAL    1.
   4.000     0.1550E+08  0.1630      0.5960E+07  0.0000E+00
LEVEL       1.   1.   0.                            ROTOR
GEOMETRY  28.
  0.0000E+00  0.0000E+00  0.0000E+00  0.3500      0.5000      0.5000      0.0000E+00  1.000
  0.0000E+00  0.0000E+00  0.0000E+00  0.4380      0.6250       1.125      0.0000E+00  1.000
  0.0000E+00  0.0000E+00  0.0000E+00   1.000      0.7000       1.000      0.0000E+00  1.000
  0.0000E+00  0.0000E+00  0.0000E+00   1.000      0.7000       1.000      0.0000E+00  1.000
  0.0000E+00  0.0000E+00  0.0000E+00  0.7500      0.7000       1.000      0.0000E+00  1.000
  0.0000E+00  0.0000E+00  0.0000E+00  0.4500      0.7000       1.000      0.0000E+00  1.000
  0.0000E+00  0.0000E+00  0.0000E+00   1.500      0.8750      0.8750      0.0000E+00  1.000
  0.0000E+00  0.0000E+00  0.0000E+00   1.500      0.8750      0.8750      0.0000E+00  1.000
  0.0000E+00  0.0000E+00  0.0000E+00   1.500      0.8750      0.8750      0.0000E+00  1.000
  0.0000E+00  0.0000E+00  0.0000E+00   1.000      0.8750      0.8750      0.0000E+00  1.000
  0.0000E+00  0.0000E+00  0.0000E+00   1.000      0.8750      0.8750      0.0000E+00  1.000
  0.0000E+00  0.0000E+00  0.0000E+00   1.000      0.8750      0.8750      0.0000E+00  1.000
  0.0000E+00  0.0000E+00  0.0000E+00   1.000      0.8750      0.8750      0.0000E+00  1.000
  0.0000E+00  0.0000E+00  0.0000E+00   1.000      0.8750      0.8750      0.0000E+00  1.000
  0.0000E+00  0.0000E+00  0.0000E+00   1.000      0.8750      0.8750      0.0000E+00  1.000
  0.0000E+00  0.0000E+00  0.0000E+00   1.000      0.8750      0.8750      0.0000E+00  1.000
  0.0000E+00  0.0000E+00  0.0000E+00   1.000      0.8750      0.8750      0.0000E+00  1.000
  0.0000E+00  0.0000E+00  0.0000E+00  0.9500      0.8750      0.8750      0.0000E+00  1.000
  0.0000E+00  0.0000E+00  0.0000E+00  0.6500       1.200       1.200      0.0000E+00  1.000
  0.0000E+00  0.0000E+00  0.0000E+00  0.9000       1.400       1.700      0.0000E+00  1.000
  0.0000E+00  0.0000E+00  0.0000E+00  0.8000       1.400       1.700      0.0000E+00  1.000
  0.0000E+00  0.0000E+00  0.0000E+00  0.5500       1.400       1.700      0.0000E+00  1.000
  0.0000E+00  0.0000E+00  0.0000E+00  0.2500       1.400       1.400      0.4375      1.000
  0,0000E+00  0.0000E+00  0.0000E+00  0.7000       1.400       1.400      0.8750      1.000
  0.0000E+00  0.0000E+00  0.0000E+00  0.3000       2.200       2.900      0.8750      1.000
  0.0000E+00  0.0000E+00  0.0000E+00  0.5000       3.600      0.1000E-01  0.0000E+00  4.000
   13.18       191.4       95.79      0.5000       1.900      0.1000E-01  0.0000E+00  4.000
  0.0000E+00  0.0000E+00  0.0000E+00  0.5000      0.8750      0.1000E-01  0.0000E+00  4.000
ACTIVE      10.
 1.   3.   5.   6.  10.  15.  21.  22.  24.  29.
LEVEL       0.   31.   2.49                         TURBINE PEDESTAL
GEOMETRY    4.
  0.0000E+00  0.0000E+00  0.0000E+00  0.3000       2.000       2.000       1.600      1.000
  0.0000E+00  0.0000E+00  0.0000E+00  0.7500     . 2.000       2.000       1.600      1.000
  0.0000E+00  0.0000E+00  0.0000E+00  0.7500       2.000       2.000       1.600      1.000
  0.0000E+00  0.0000E+00  0.0000E+00  0.3000       2.000       2.000       1.600      1.000
ACTIVE      5.
31.  32.  33.  34.  35.
LEVEL       0.   41.   18.3                         DISK PEDESTAL
GEOMETRY    5.
  0.0000E+00  0.0000E+00  0.0000E+00  0.3500       3.000       3.000       2.550      1.000
  0.0000E+00  0.0000E+00  0.0000E+00  0.3500       3.000       3.000       2.550      1.000
  0.0000E+00  0.0000E+00  0.0000E+00  0.8000       3.000       3.000       2.550      1.000
  0.0000E+00  0.0000E+00  0.0000E+00  0.3500       3.000       3.000       2.550      1.000
  0.0000E+00  0.0000E+00  0.0000E+00  0.3500       3.000       3.000       2.550      1.000
ACTIVE      6.
41.  42.  43.  44.  45.  46.
SYSTEM
```

TEST RIG MODEL

```
*****************************************************************************
*                PROGRAM STATUS       (VERSION 2.0   1-18-85)                *
*****************************************************************************
*                                                                           *
*  NUMBER OF LEVELS  - - - - - -  3     DEBUG OPTIONS                       *
*  NUMBER OF STATIONS  - - - - - 40       NBUG1 =    0 BASIC DEBUG          *
*  NUMBER OF BEARINGS  - - - - -  8       NBUG2 =    0 ELEMENT FORMULATION  *
*  NO. OF USER INPUT MATERIALS -  1       NBUG3 =    0 BLOCK-STODOLA ITERATION *
*  NO. OF DEGREES-OF-FREEDOM - -160       NBUG4 =    0 MATH ROUTINES        *
*                                                                           *
*                                                                           *
*****************************************************************************
```

```
*************************************************************
*                      OPTIONS IN EFFECT                    *
*************************************************************
*                                                           *
*   CRIT    - CRITICAL SPEEDS CALCULATION                   *
*   UNIT    - AMERICAN                                      *
*   POST    - SPECIAL OUTPUT FILE FOR POST PLOT WILL BE     *
*             GENERATED, 'ALL' STATIONS INVOKED             *
*   TIMO    - TIMOSHENKO BEAM                               *
*                                                           *
*************************************************************
```

```
*************************************************************
*      DIMENSION REQUIRED FOR THE  3  GLOBAL ARRAYS         *
*                                                           *
*                              IG        GR        GC       *
*    PROBLEM FORMULATION       641      3781      5441      *
*    AVAILABLE - - - - -      2000      8000     80000      *
*                                                           *
*************************************************************
```

*** MTI *** DYNAMIC ANALYSIS OF ROTOR-BEARING SYSTEMS VERSION 2.0 1-18-85 MECHANICAL TECHNOLOGY INC.

TEST RIG MODEL

****
* SUMMARY OF LEVEL NO. 1 * ROTOR *
****

*TYPE OF ELEMENT - BEAM *NUMBER.OF ROTOR SEGMENTS - 28 *SPEED RATIO - 1.00 *STARTING AXIAL LOCATION - 0.000

1. SHAFT GEOMETRY

ROTOR BTWN.		SEGMENT STATIONS	SEGMENT LENGTH (IN)	STIFFNESS DIAMETER (IN)	MASS DIAMETER (IN)	INNER DIAMETER (IN)	MATERIAL NUMBER
1	AND	2	0.3500	0.5000	0.5000	0.0000	1.
2	AND	3	0.4380	0.6250	1.1250	0.0000	1.
3	AND	4	1.0000	0.7000	1.0000	0.0000	1.
4	AND	5	1.0000	0.7000	1.0000	0.0000	1.
5	AND	6	0.7500	0.7000	1.0000	0.0000	1.
6	AND	7	0.4500	0.7000	1.0000	0.0000	1.
7	AND	8	1.5000	0.8750	0.8750	0.0000	1.
8	AND	9	1.5000	0.8750	0.8750	0.0000	1.
9	AND	10	1.5000	0.8750	0.8750	0.0000	1.
10	AND	11	1.0000	0.8750	0.8750	0.0000	1.
11	AND	12	1.0000	0.8750	0.8750	0.0000	1.
12	AND	13	1.0000	0.8750	0.8750	0.0000	1.
13	AND	14	1.0000	0.8750	0.8750	0.0000	1.
14	AND	15	1.0000	0.8750	0.8750	0.0000	1.
15	AND	16	1.0000	0.8750	0.8750	0.0000	1.
16	AND	17	1.0000	0.8750	0.8750	0.0000	1.
17	AND	18	1.0000	0.8750	0.8750	0.0000	1.
18	AND	19	0.9500	0.8750	0.8750	0.0000	1.
19	AND	20	0.6500	1.2000	1.2000	0.0000	1.
20	AND	21	0.9000	1.4000	1.7000	0.0000	1.
21	AND	22	0.8000	1.4000	1.7000	0.0000	1.
22	AND	23	0.5500	1.4000	1.7000	0.0000	1.
23	AND	24	0.2500	1.4000	1.4000	0.4375	1.
24	AND	25	0.7000	1.4000	1.4000	0.8750	1.
25	AND	26	0.3000	2.2000	2.9000	0.8750	1.
26	AND	27	0.5000	3.6000	0.0100	0.0000	4.
27	AND	28	0.5000	1.9000	0.0100	0.0000	4.
28	AND	29	0.5000	0.8750	0.0100	0.0000	4.
	TOTAL		23.0879				

2 LUMPED MASS DATA

	MASS	IT	IP	ECC	ANGLE

	(LB)	(LB-IN**2)	(LB-IN**2)	(IN)	(DEG)
27	13.18	95.79	191.4	0.0000E+00	0.0000E+00

!!NO SHAFT ECCENTRICITY SPECIFIED IN CARD GROUP 3

TEST RIG MODEL

****
* SUMMARY OF LEVEL NO. 2 * TURBINE PEDESTAL *
****

*TYPE OF ELEMENT - BEAM *NUMBER OF ROTOR SEGMENTS - 4 *SPEED RATIO - 0.00 *STARTING AXIAL LOCATION - 2.490

1. SHAFT GEOMETRY

ROTOR SEGMENT BTWN. STATIONS			SEGMENT LENGTH (IN)	STIFFNESS DIAMETER (IN)	MASS DIAMETER (IN)	INNER DIAMETER (IN)	MATERIAL NUMBER
31	AND	32	0.3000	2.0000	2.0000	1.6000	1.
32	AND	33	0.7500	2.0000	2.0000	1.6000	1.
33	AND	34	0.7500	2.0000	2.0000	1.6000	1.
34	AND	35	0.3000	2.0000	2.0000	1.6000	1.
		TOTAL	2.1000				

!!NO LUMPED MASS SPECIFIED IN CARD GROUP 3

!!NO SHAFT ECCENTRICITY SPECIFIED IN CARD GROUP 3

*** MTI *** DYNAMIC ANALYSIS OF ROTOR-BEARING SYSTEMS VERSION 2.0 1-18-85 MECHANICAL TECHNOLOGY INC.

TEST RIG MODEL

****
* SUMMARY OF LEVEL NO. 3 * DISK PEDESTAL *
****

*TYPE OF ELEMENT - BEAM *NUMBER OF ROTOR SEGMENTS - 5 *SPEED RATIO - 0.00 *STARTING AXIAL LOCATION - 18.300

1. SHAFT GEOMETRY

ROTOR BTWN.		SEGMENT STATIONS	SEGMENT LENGTH (IN)	STIFFNESS DIAMETER (IN)	MASS DIAMETER (IN)	INNER DIAMETER (IN)	MATERIAL NUMBER
41	AND	42	0.3500	3.0000	3.0000	2.5500	1.
42	AND	43	0.3500	3.0000	3.0000	2.5500	1.
43	AND	44	0.8000	3.0000	3.0000	2.5500	1.
44	AND	45	0.3500	3.0000	3.0000	2.5500	1.
45	AND	46	0.3500	3.0000	3.0000	2.5500	1.
		TOTAL	2.2000				

!!NO LUMPED MASS SPECIFIED IN CARD GROUP 3

!!NO SHAFT ECCENTRICITY SPECIFIED IN CARD GROUP 3

ELEMENT MATRICES WERE STORED ON LOGICAL UNIT 2

TEST RIG MODEL

****

* SUMMARY OF LEVEL NO. 1 * ROTOR * .....CALCULATED OUTPUT

****

ROTOR BTWN.		SEGMENT STATIONS	ACC LEN (IN)	EI LB-IN**2	MASS (LB)	IT LB-IN**2	IP LB-IN**2	SHAPE FACTOR
1	AND	2	0.3500	0.920E+05	0.194E-01	0.502E-03	0.608E-03	0.886
2	AND	3	0.7880	0.225E+06	0.123	0.117E-01	0.195E-01	0.886
3	AND	4	1.7880	0.354E+06	0.222	0.324E-01	0.278E-01	0.886
4	AND	5	2.7880	0.354E+06	0.222	0.324E-01	0.278E-01	0.886
5	AND	6	3.5380	0.354E+06	0.167	0.182E-01	0.208E-01	0.886
6	AND	7	3.9880	0.354E+06	0.100	0.794E-02	0.125E-01	0.886
7	AND	8	5.4880	0.863E+06	0.255	0.601E-01	0.244E-01	0.886
8	AND	9	6.9880	0.863E+06	0.255	0.601E-01	0.244E-01	0.886
9	AND	10	8.4880	0.863E+06	0.255	0.601E-01	0.244E-01	0.886
10	AND	11	9.4880	0.863E+06	0.170	0.223E-01	0.163E-01	0.886
11	AND	12	10.4880	0.863E+06	0.170	0.223E-01	0.163E-01	0.886
12	AND	13	11.4880	0.863E+06	0.170	0.223E-01	0.163E-01	0.886
13	AND	14	12.4880	0.863E+06	0.170	0.223E-01	0.163E-01	0.886
14	AND	15	13.4880	0.863E+06	0.170	0.223E-01	0.163E-01	0.886
15	AND	16	14.4880	0.863E+06	0.170	0.223E-01	0.163E-01	0.886
16	AND	17	15.4880	0.863E+06	0.170	0.223E-01	0.163E-01	0.886
17	AND	18	16.4880	0.863E+06	0.170	0.223E-01	0.163E-01	0.886
18	AND	19	17.4380	0.863E+06	0.162	0.199E-01	0.155E-01	0.886
19	AND	20	18.0880	0.305E+07	0.208	0.260E-01	0.374E-01	0.886
20	AND	21	18.9880	0.566E+07	0.578	0.143	0.209	0.886
21	AND	22	19.7880	0.566E+07	0.514	0.120	0.186	0.886
22	AND	23	20.3380	0.566E+07	0.353	0.727E-01	0.128	0.886
23	AND	24	20.5880	0.560E+07	0.983E-01	0.137E-01	0.264E-01	0.728
24	AND	25	21.2879	0.479E+07	0.186	0.392E-01	0.633E-01	0.575
25	AND	26	21.5879	0.336E+08	0.510	0.296	0.585	0.673
26	AND	27	22.0879	0.128E+09	0.640E-05	0.133E-06	0.800E-10	0.886
27	AND	28	22.5879	0.992E+07	0.640E-05	0.133E-06	0.800E-10	0.886
28	AND	29	23.0879	0.446E+06	0.640E-05	0.133E-06	0.800E-10	0.886

*** MTI *** DYNAMIC ANALYSIS OF ROTOR-BEARING SYSTEMS VERSION 2.0 1-18-85 MECHANICAL TECHNOLOGY INC.

TEST RIG MODEL

ROTOR BTWN.	SEGMENT STATIONS	ACC LEN (IN)	EI LB-IN**2	MASS (LB)	IT LB-IN**2	IP LB-IN**2	SHAPE FACTOR
SUMMARY OF LEVEL NO. 2 *	TURBINE PEDESTAL *				.....CALCULATED OUTPUT		
31	AND 32	2.7900	0.139E+08	0.960E-01	0.401E-01	0.787E-01	0.541
32	AND 33	3.5400	0.139E+08	0.240	0.110	0.197	0.541
33	AND 34	4.2900	0.139E+08	0.240	0.110	0.197	0.541
34	AND 35	4.5900	0.139E+08	0.960E-01	0.401E-01	0.787E-01	0.541

TEST RIG MODEL

* SUMMARY OF LEVEL NO. 3 * DISK PEDESTAL *						.....CALCULATED OUTPUT	
ROTOR BTWN.	SEGMENT STATIONS	ACC LEN (IN)	EI LB-IN**2	MASS (LB)	IT LB-IN**2	IP LB-IN**2	SHAPE FACTOR
41	AND 42	18.6500	0.570E+08	0.194	0.190	0.376	0.536
42	AND 43	19.0000	0.570E+08	0.194	0.190	0.376	0.536
43	AND 44	19.8000	0.570E+08	0.444	0.454	0.861	0.536
44	AND 45	20.1500	0.570E+08	0.194	0.190	0.376	0.536
45	AND 46	20.5000	0.570E+08	0.194	0.190	0.376	0.536

TEST RIG MODEL

****
* MATERIAL SUMMARY *
****

MATERIAL NUMBER	MODULUS OF ELASTICITY (LB/IN**2)	DENSITY (LB/IN**3)	SHEAR MODULUS (LB/IN**2)	POISSON'S RATIO
1	0.3000E+08	0.2830	0.1100E+08	0.3000
4	0.1550E+08	0.1630	0.5960E+07	0.3003

POISSON'S RATIO WILL BE CALCULATED BY THE PROGRAM IF NOT SPECIFIED

****
* SUMMARY OF STATIC CONDENSATION *
****

ACTIVE STATIONS SELECTED ON LEVEL - 1 2 3
NO. OF ACTIVE STATIONS - 10 5 6
NO. OF ACTIVE PEDESTAL STATIONS- 0 0 0

STATION NO.	1	3	5	6	10	15	21	22	24	29	31	32	33	34	35	41	42	43	44	45	46
D-O-F	4	4	4	4	4	4	4	4	4	4	4	4	4	4	4	4	4	4	4	4	4

SYSTEM BEFORE STATIC CONDENSATION
NUMBER OF STATIONS - - - - - - 40
NUMBER OF DEGREES OF FREEDOM - 160

SYSTEM AFTER STATIC CONDENSATION
NUMBER OF ACTIVE STATIONS - - 21
NUMBER OF D-O-F (FIXED FRAME) - 84
NUMBER OF D-O-F (WHIRL FRAME) - 42

```
*** MTI ***  DYNAMIC ANALYSIS OF ROTOR-BEARING SYSTEMS   VERSION 2.0   1-18-85       MECHANICAL TECHNOLOGY INC.

  TEST RIG MODEL


READ -SYST- FROM INPUT ...START TO READ SYSTEM PROPERTIES
READ CARD GROUP 4  --ECHO OF INPUT

MASS        4.
    3.  0.0000E+00  0.0000E+00  0.0000E+00 -0.3000E-02   30.00
   10.  0.0000E+00  0.0000E+00  0.0000E+00 -0.3000E-03   150.0
   15.  0.0000E+00  0.0000E+00  0.0000E+00 -0.3000E-03   210.0
   29.  0.0000E+00  0.0000E+00  0.0000E+00 -0.8000E-02   330.0
IC
PLANES      3.
    10.    22.    29.
     1.     1.     1.
PROBES      3.
    10.    22.    29.
     1.     1.     1.
COEFF
BEARING     5.    32.   1.    0.
  0.0000E+00  0.3000E+07  0.0000E+00  0.0000E+00  0.3000E+07  0.0000E+00  0.0000E+00  0.0000E+00  0.0000E+00
BEARING     6.    33.  -1.    0.
BEARING    32.    0.    1.    0.
  0.0000E+00  0.7500E+05  0.0000E+00  0.0000E+00  0.7500E+05   1.000      0.0000E+00  0.0000E+00   1.000
BEARING    34.    0.   -3.    0.
BEARING    21.    43.  -1.    0.
BEARING    22.    44.  -1.    0.
BEARING    42.    0.    1.    0.
  0.0000E+00   9000.       0.0000E+00  0.0000E+00   9000.       1.000      0.0000E+00  0.0000E+00   1.000
BEARING    45.    0.    1.    0.
  0.0000E+00   9000.       0.0000E+00  0.0000E+00   9000.       1.000      0.0000E+00  0.0000E+00   1.000
SPEED      -1.   1.
  0.0000E+00
```

TEST RIG MODEL

****
* SYSTEM SUMMARY - SYSTEM CONDITION 1 *
****

1. SYSTEM LUMPED MASS

STATION NUMBER	LUMPED MAS (LB)	IT (LB-IN**2)	IP (LB-IN**2)	ECC (IN)	ANGLE (DEG)
3.	0.0000E+00	0.0000E+00	0.0000E+00	-0.3000E-02	30.00
10.	0.0000E+00	0.0000E+00	0.0000E+00	-0.3000E-03	150.0
15.	0.0000E+00	0.0000E+00	0.0000E+00	-0.3000E-03	210.0
29.	0.0000E+00	0.0000E+00	0.0000E+00	-0.8000E-02	330.0

2. TOTAL MASS, IP AND CENTER OF GRAVITY (CALCULATED)

LEVEL	SUB	TITLE	MASS (LB)	TOTAL IP (LB-IN**2)	C. G. (IN)	
1		ROTOR	18.77	193.0	19.48	0.4096E+05
2		TURBINE PEDESTAL	0.6721	0.5512	3.540	0.5226
3		DISK PEDESTAL	1.221	2.367	19.40	1.677

READ - LOT- FROM INPUT ...IGNORED

READ - MEG- FROM INPUT ...IGNORED

READ - MPL- FROM INPUT ...IGNORED

TEST RIG MODEL

3. DYNAMICAL SUPPORT COEFFICIENTS

LATERAL COEFFICIENTS (TRANSLATIONAL)

STATION	SPEED	KXX (LB/IN)	KXY (LB/IN)	KYX (LB/IN)	KYY (LB/IN)	CXX (LB-S/IN)	CXY (LB-S/IN)	CYX (LB-S/IN)	CYY (LB-S/IN)
5 AND 32	- -	0.3000E+07	0.0000E+00	0.0000E+00	0.3000E+07	0.0000E+00	0.0000E+00	0.0000E+00	0.0000E+00
6 AND 33	- -	0.3000E+07	0.0000E+00	0.0000E+00	0.3000E+07	0.0000E+00	0.0000E+00	0.0000E+00	0.0000E+00
32 AND 0	- -	0.7500E+05	0.0000E+00	0.0000E+00	0.7500E+05	1.000	0.0000E+00	0.0000E+00	1.000
34 AND 0	- -	0.7500E+05	0.0000E+00	0.0000E+00	0.7500E+05	1.000	0.0000E+00	0.0000E+00	1.000
21 AND 43	- -	0.3000E+07	0.0000E+00	0.0000E+00	0.3000E+07	0.0000E+00	0.0000E+00	0.0000E+00	0.0000E+00
22 AND 44	- -	0.3000E+07	0.0000E+00	0.0000E+00	0.3000E+07	0.0000E+00	0.0000E+00	0.0000E+00	0.0000E+00
42 AND 0	- -	9000.	0.0000E+00	0.0000E+00	9000.	1.000	0.0000E+00	0.0000E+00	1.000
45 AND 0	- -	9000.	0.0000E+00	0.0000E+00	9000.	1.000	0.0000E+00	0.0000E+00	1.000

NO ANGULAR COEFFICIENT SPECIFIED

READ -EXEC- FROM INPUT ...START TO EXECUTE

!!DIMENSION OF 18407 IS REQUIRED FOR MATRIX GC

TEST RIG MODEL

****
* CRITICAL SPEEDS ANALYSIS *
****

****
* SYSTEM CONDITION 1 *
****

FREQUENCY RANGE REQUESTED
LOWER BOUND (RPM) = 0.00000E+00
UPPER BOUND (RPM) = 50000.

***SYSTEM WHIRL SPEED RATIO = 1.00 ***

- SPIN SPEED RATIO -		
LEVEL	1	1.00
LEVEL	2	0.00
LEVEL	3	0.00

- - - - - - -SYSTEM SPIN-SPEED-DEPENDENT SUPPORT COEFFICIENTS - - - - - - -

--LATERAL COEFFICIENTS AT ROTATIONAL SPEED

STA.	NO.	KXX (LB/IN)	KXY (LB/IN)	KYX (LB/IN)	KYY (LB/IN)	CXX (LB-S/IN)	CXY (LB-S/IN)	CYX (LB-S/IN)	CYY (LB-S/IN)
5. AND	32.	0.3000E+07	0.0000E+00	0.0000E+00	0.3000E+07				
6. AND	33.	0.3000E+07	0.0000E+00	0.0000E+00	0.3000E+07				
32. AND	0.	0.7500E+05	0.0000E+00	0.0000E+00	0.7500E+05				
34. AND	0.	0.7500E+05	0.0000E+00	0.0000E+00	0.7500E+05				
21. AND	43.	0.3000E+07	0.0000E+00	0.0000E+00	0.3000E+07				
22. AND	44.	0.3000E+07	0.0000E+00	0.0000E+00	0.3000E+07				
42. AND	0.	9000.	0.0000E+00	0.0000E+00	9000.				
45. AND	0.	9000.	0.0000E+00	0.0000E+00	9000.				

--NO ANGULAR COEFFICIENT SPECIFIED

TEST RIG MODEL

****
* SYSTEM CRITICAL SPEED SUMMARY *
****

	NATURAL FREQUENCIES (RPM)	(RPS)	(RAD/S)
1	4967.3	82.789	520.18
2	23550.	392.50	2466.1
3	40949.	682.48	4288.1

3 NATURAL FREQUENCIES WITHIN THE RANGE SPECIFIED

*** MTI *** DYNAMIC ANALYSIS OF ROTOR-BEARING SYSTEMS VERSION 2.0 1-18-85 MECHANICAL TECHNOLOGY INC.

TEST RIG MODEL

MODE # 1 LEVEL # 1 ROTOR

NORMALIZED AMPLITUDE

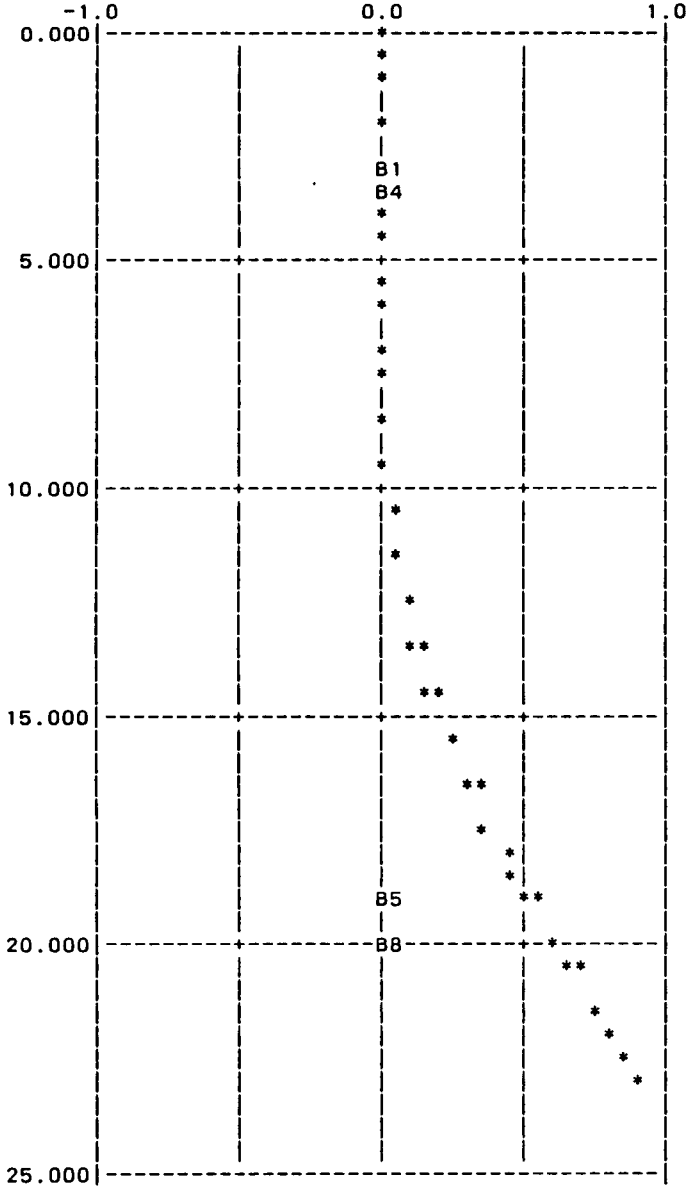

STA.	AT (IN)	AMPLITUDE
1	0.000	0.0014
2	0.350	0.0006
3	0.788	-0.0003
4	1.788	-0.0026
5	2.788	-0.0048
6	3.538	-0.0065
7	3.988	-0.0077
8	5.488	-0.0104
9	6.988	-0.0089
10	8.488	0.0004
11	9.488	0.0126
12	10.488	0.0309
13	11.488	0.0563
14	12.488	0.0899
15	13.488	0.1326
16	14.488	0.1857
17	15.488	0.2500
18	16.488	0.3269
19	17.438	0.4126
20	18.088	0.4766
21	18.988	0.5675
22	19.788	0.6502
24	20.588	0.7346
26	21.588	0.8406
27	22.088	0.8936
28	22.588	0.9467
29	23.088	1.0000

BRG # 1 AT 5 & 32
KXX= 0.30E+07

BRG # 2 AT 6 & 33
KXX= 0.30E+07

BRG # 5 AT 21 & 43
KXX= 0.30E+07

BRG # 6 AT 22 & 44
KXX= 0.30E+07

MODE # 1 CRITICAL SPEED 4967.33 RPM

TEST RIG MODEL

MODE # 1 LEVEL # 2 TURBINE PEDESTAL

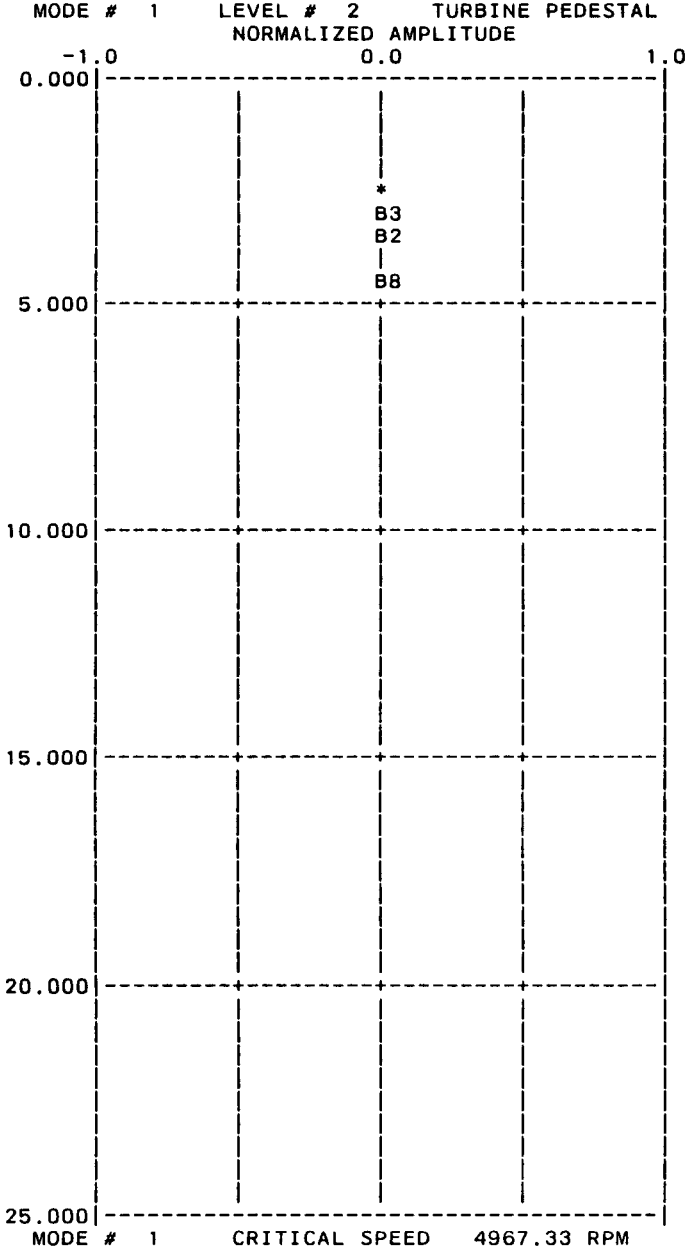

STA.	AT (IN)	AMPLITUDE
31	2.490	-0.0044
32	2.790	-0.0049
33	3.540	-0.0061
35	4.590	-0.0077

BRG # 1 AT 5 & 32
KXX= 0.30E+07

BRG # 2 AT 6 & 33
KXX= 0.30E+07

BRG # 3 AT 32 & 0
KXX= 0.75E+05

BRG # 4 AT 34 & 0
KXX= 0.75E+05

MODE # 1 CRITICAL SPEED 4967.33 RPM

TEST RIG MODEL

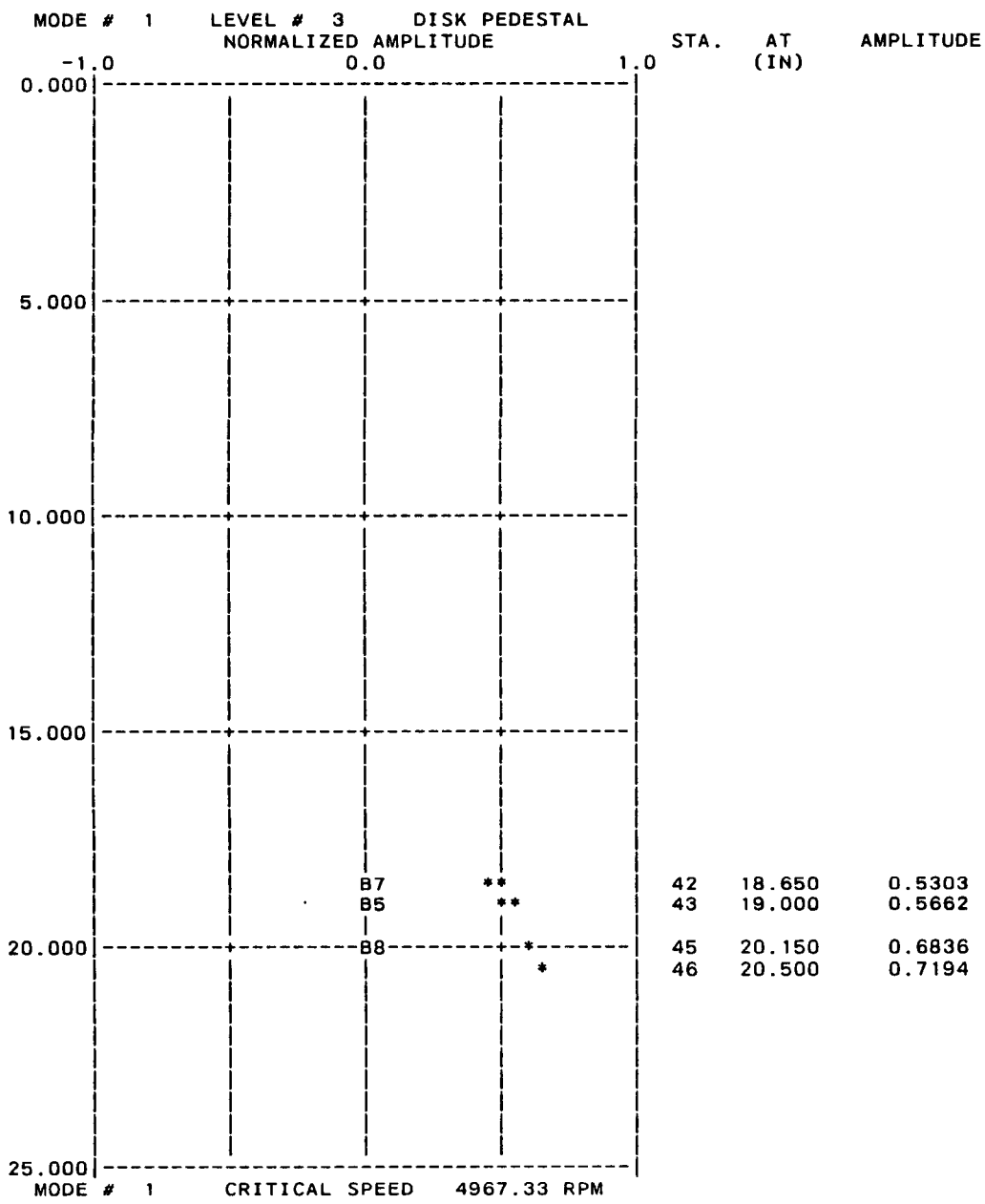

STA.	AT (IN)	AMPLITUDE
42	18.650	0.5303
43	19.000	0.5662
45	20.150	0.6836
46	20.500	0.7194

BRG # 5 AT 21 & 43
KXX= 0.30E+07

BRG # 6 AT 22 & 44
KXX= 0.30E+07

BRG # 7 AT 42 & 0
KXX= 0.90E+04

BRG # 8 AT 45 & 0
KXX= 0.90E+04

TEST RIG MODEL

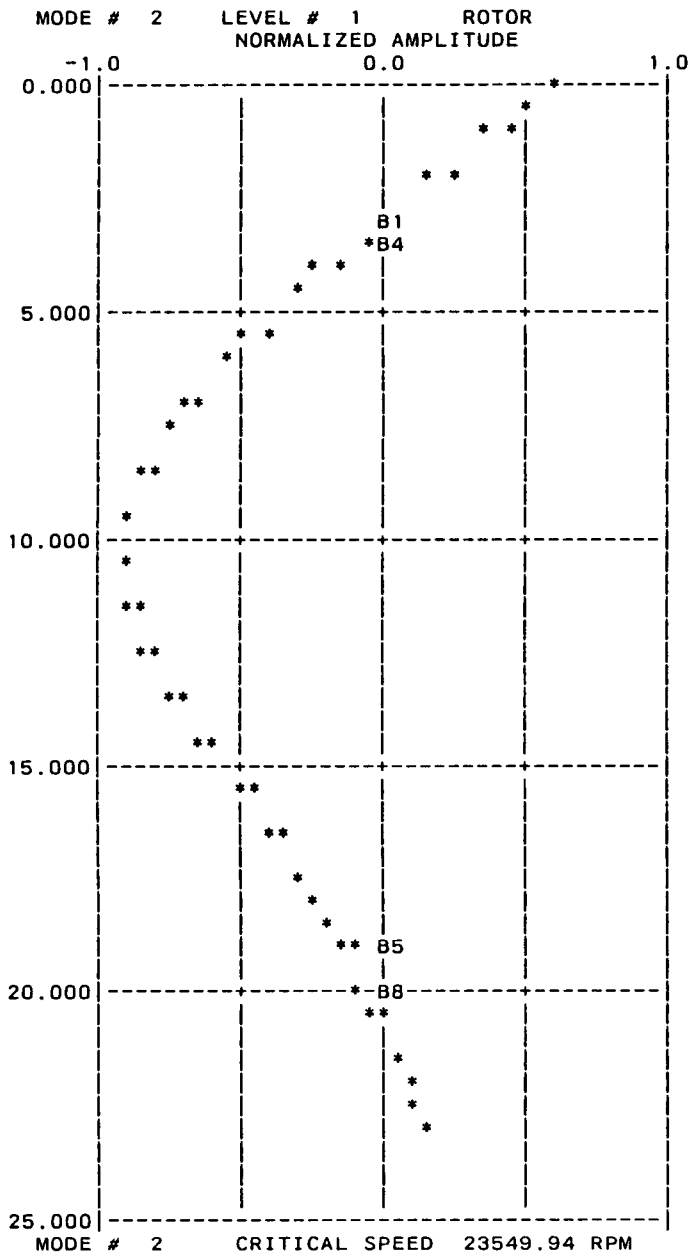

MODE # 2 CRITICAL SPEED 23549.94 RPM

STA.	AT (IN)	AMPLITUDE
1	0.000	0.6475
2	0.350	0.5746
3	0.788	0.4835
4	1.788	0.2761
5	2.788	0.0753
6	3.538	-0.0664
7	3.988	-0.1562
8	5.488	-0.4499
9	6.988	-0.7096
10	8.488	-0.9010
11	9.488	-0.9729
12	10.488	-1.0000
13	11.488	-0.9851
14	12.488	-0.9312
15	13.488	-0.8411
16	14.488	-0.7192
17	15.488	-0.5819
18	16.488	-0.4439
19	17.438	-0.3258
20	18.088	-0.2550
21	18.988	-0.1627
22	19.788	-0.0860
24	20.588	-0.0166
26	21.588	0.0555
27	22.088	0.0915
28	22.588	0.1267
29	23.088	0.1568

BRG # 1 AT 5 & 32
KXX= 0.30E+07

BRG # 2 AT 6 & 33
KXX= 0.30E+07

BRG # 5 AT 21 & 43
KXX= 0.30E+07

BRG # 6 AT 22 & 44
KXX= 0.30E+07

TEST RIG MODEL

MODE # 2 LEVEL # 2 TURBINE PEDESTAL

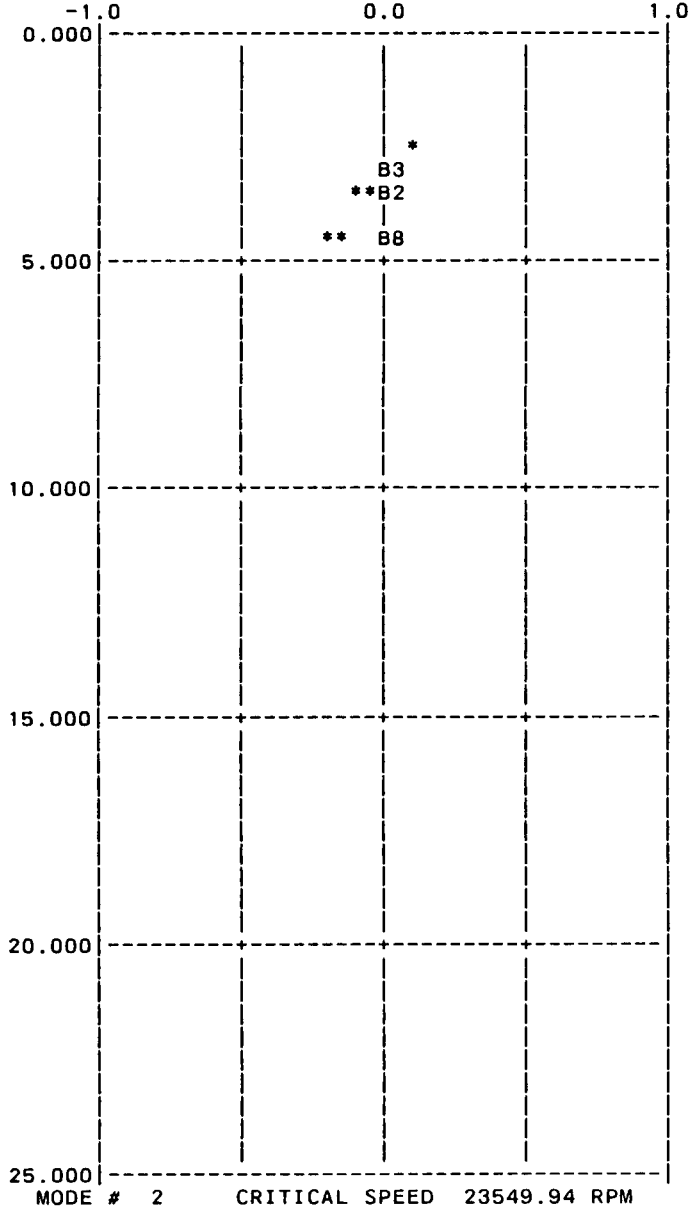

STA.	AT (IN)	AMPLITUDE
31	2.490	0.1198
32	2.790	0.0694
33	3.540	-0.0579
35	4.590	-0.2323

BRG # 1 AT 5 & 32
KXX= 0.30E+07

BRG # 2 AT 6 & 33
KXX= 0.30E+07

BRG # 3 AT 32 & 0
KXX= 0.75E+05

BRG # 4 AT 34 & 0
KXX= 0.75E+05

MODE # 2 CRITICAL SPEED 23549.94 RPM

TEST RIG MODEL

MODE # 2 LEVEL # 3 DISK PEDESTAL

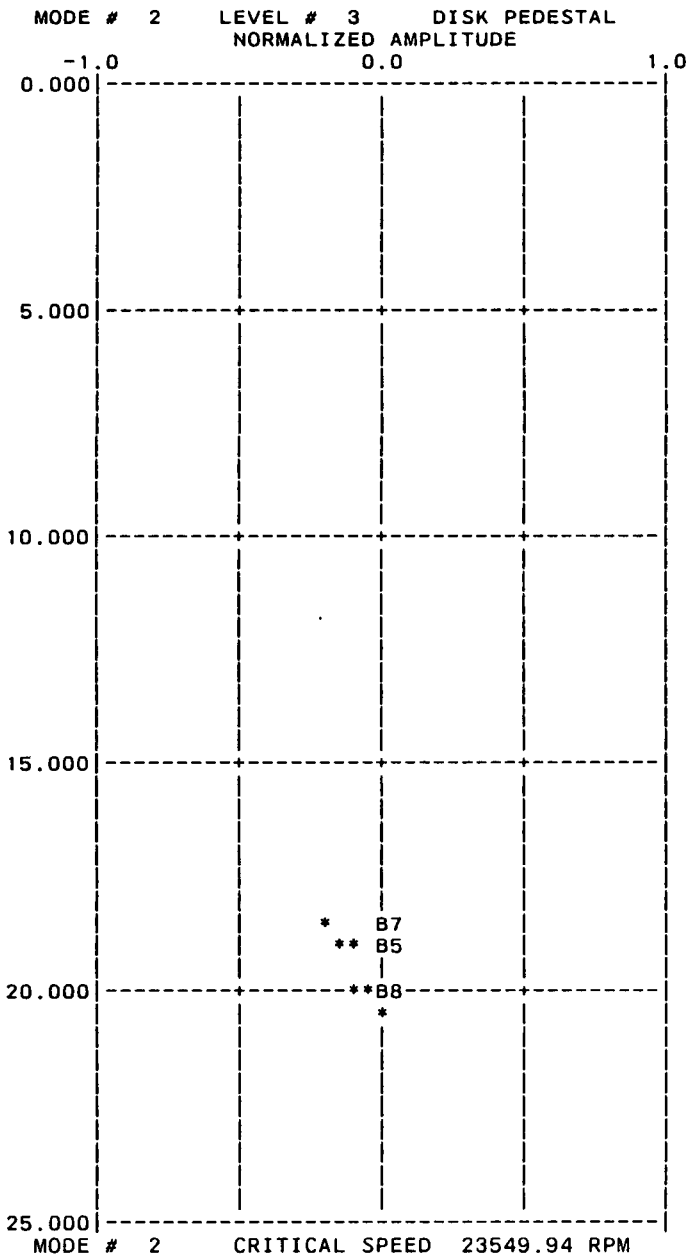

STA.	AT (IN)	AMPLITUDE
42	18.650	-0.1962
43	19.000	-0.1627
45	20.150	-0.0525
46	20.500	-0.0189

BRG # 5 AT 21 & 43
KXX= 0.30E+07

BRG # 6 AT 22 & 44
KXX= 0.30E+07

BRG # 7 AT 42 & 0
KXX= 0.90E+04

BRG # 8 AT 45 & 0
KXX= 0.90E+04

MODE # 2 CRITICAL SPEED 23549.94 RPM

TEST RIG MODEL

MODE # 3 LEVEL # 1 ROTOR

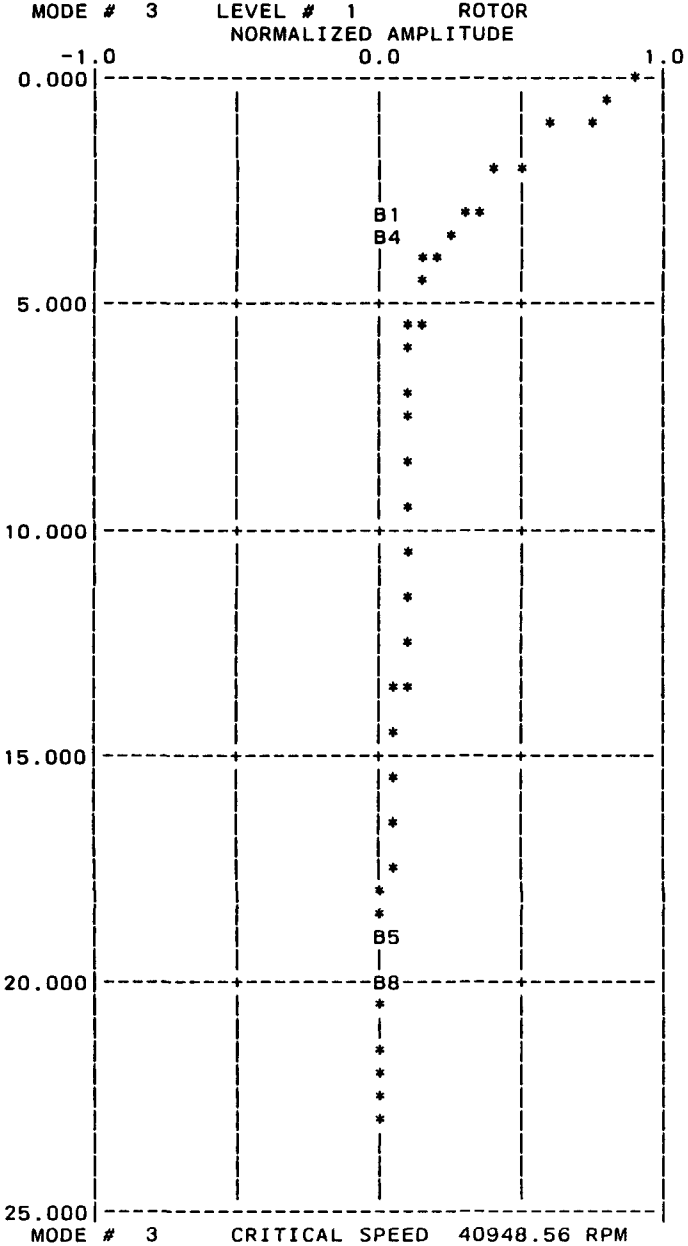

STA.	AT (IN)	AMPLITUDE
1	0.000	1.0000
2	0.350	0.9150
3	0.788	0.8092
4	1.788	0.5707
5	2.788	0.3667
6	3.538	0.2596
7	3.988	0.2190
8	5.488	0.1404
9	6.988	0.1091
10	8.488	0.1024
11	9.488	0.1011
12	10.488	0.1001
13	11.488	0.0981
14	12.488	0.0935
15	13.488	0.0851
16	14.488	0.0719
17	15.488	0.0566
18	16.488	0.0413
19	17.438	0.0289
20	18.088	0.0219
21	18.988	0.0131
22	19.788	0.0062
24	20.588	0.0005
26	21.588	-0.0040
27	22.088	-0.0062
28	22.588	-0.0082
29	23.088	-0.0094

BRG # 1 AT 5 & 32
KXX= 0.30E+07

BRG # 2 AT 6 & 33
KXX= 0.30E+07

BRG # 5 AT 21 & 43
KXX= 0.30E+07

BRG # 6 AT 22 & 44
KXX= 0.30E+07

MODE # 3 CRITICAL SPEED 40948.56 RPM

TEST RIG MODEL

MODE # 3 LEVEL # 2 TURBINE PEDESTAL

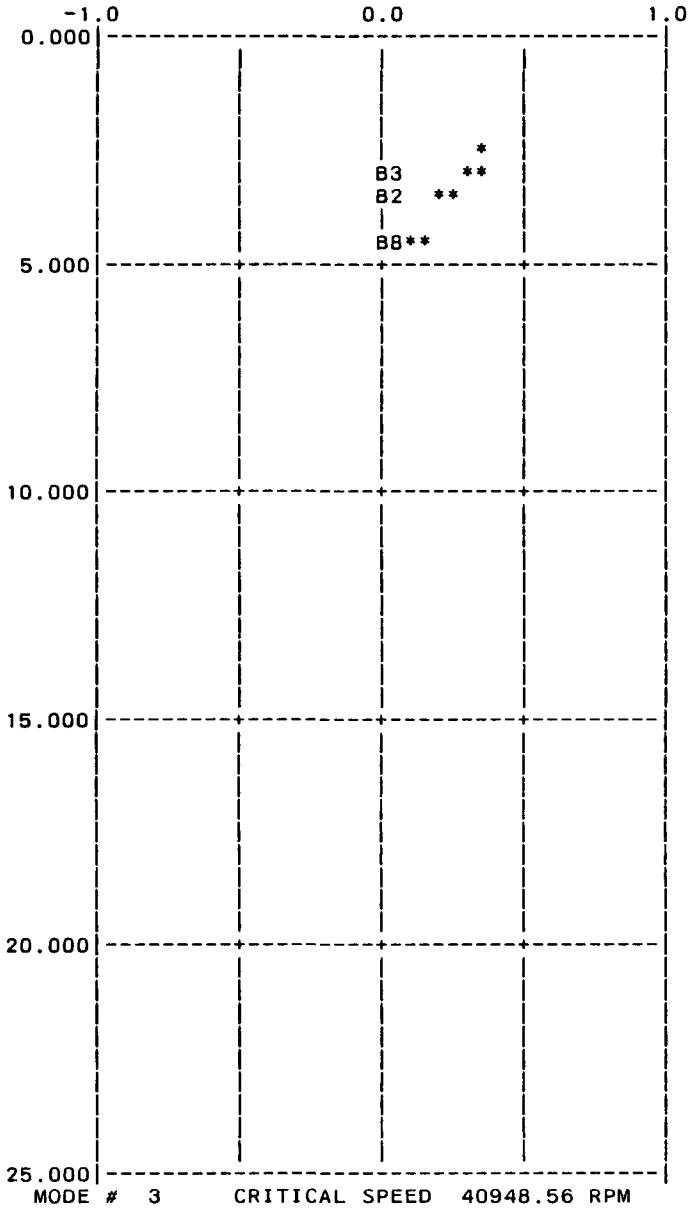

STA.	AT (IN)	AMPLITUDE
31	2.490	0.4059
32	2.790	0.3622
33	3.540	0.2541
35	4.590	0.1000

BRG # 1 AT 5 & 32
KXX= 0.30E+07

BRG # 2 AT 6 & 33
KXX= 0.30E+07

BRG # 3 AT 32 & 0
KXX= 0.75E+05

BRG # 4 AT 34 & 0
KXX= 0.75E+05

MODE # 3 CRITICAL SPEED 40948.56 RPM

TEST RIG MODEL

MODE # 3 LEVEL # 3 DISK PEDESTAL

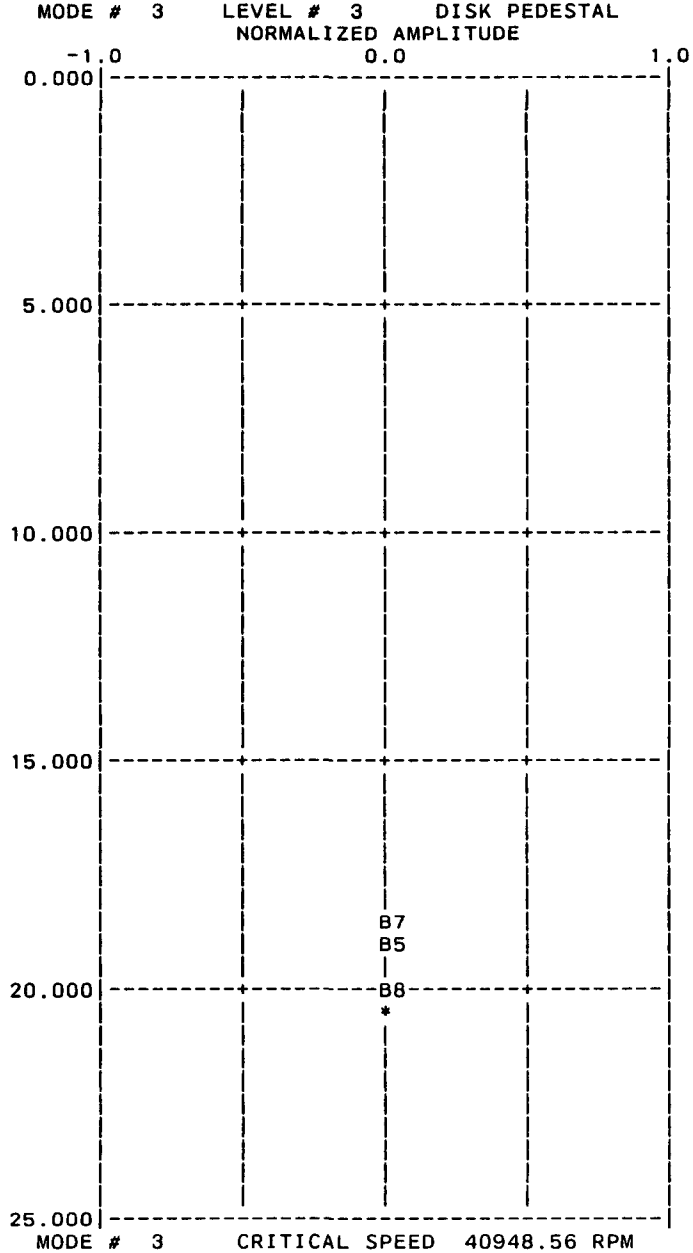

STA.	AT (IN)	AMPLITUDE
42	18.650	0.0164
43	19.000	0.0133
45	20.150	0.0030
46	20.500	-0.0001

BRG # 5 AT 21 & 43
KXX= 0.30E+07

BRG # 6 AT 22 & 44
KXX= 0.30E+07

BRG # 7 AT 42 & 0
KXX= 0.90E+04

BRG # 8 AT 45 & 0
KXX= 0.90E+04

MODE # 3 CRITICAL SPEED 40948.56 RPM

TOTAL EXECUTION TIME 19.9 SEC